

Solubility Classification of Airborne Uranium Products from LWR-Fuel Plants

Manuscript Completed: July 1980
Date Published: August 1980

Prepared by
D. R. Kalkwarf

Pacific Northwest Laboratory
Richland, WA 99352

Prepared for
Division of Siting, Health and Safeguards Standards
Office of Standards Development
U.S. Nuclear Regulatory Commission
Washington, D.C. 20555
NRC FIN No. B21239

8009260688

ABSTRACT

Airborne dust samples were obtained from various locations within plants manufacturing fuel elements for light-water reactors, and the dissolution rates of uranium from these samples into simulated lung fluid at 37°C were measured. These measurements were used to classify the solubilities of the samples in terms of the lung clearance model proposed by the International Commission on Radiological Protection. Similar evaluations were performed for samples of pure uranium compounds expected as components in plant dust. The variation in solubility classifications of dust encountered along the fuel production lines is described and correlated with the process chemistry and the solubility classifications of the pure uranium compounds.

SOLUBILITY CLASSIFICATION OF AIRBORNE URANIUM PRODUCTS FROM LWR-FUEL PLANTS

EXECUTIVE SUMMARY

Airborne uranium dust samples were obtained from several locations within each of four plants manufacturing fuel elements for light-water reactors, and the dissolution rates of these mixtures and their pure components were classified in terms of the ICRP Task Group Lung Model. Each sample was exposed to well-agitated quantities of simulated lung fluid at 37°C, and classification was based on the fraction, F , of uranium remaining undissolved as a function of time. In order to allow for the presence of more than one type of uranium compound in a sample, this functional dependence was represented by a sum of exponential terms, i.e.,

$$F = \sum_i f_i \exp(-0.693 t/T_i)$$
, where f_i is the initial weight fraction of component i and T_i is its dissolution half-time. Based on such measurements, the following classifications are recommended for pure uranium compounds expected as dust components in the plants: $(\text{NH}_4)_2\text{U}_2\text{O}_7$ - D; UO_3 - 48%, 52% Y; UF_4 - Y; U_3O_8 - Y; and UO_2 - Y. The dissolution-rate classifications of plant dust generally were in agreement with expectations based on process chemistry at a sample-collection site and the classifications of the pure compounds expected at that site. They varied with distance along the processing lines from largely D at the UF_6 vaporizers to entirely Y where the finished pellets are ground to size. Dissolution of the uranium-bearing components was shown to be the result of reaction with bicarbonate ion to form the soluble $[\text{UO}_2(\text{CO}_3)_3]^{4-}$ anion.

TABLE OF CONTENTS

ABSTRACT	iii
EXECUTIVE SUMMARY.	v
TABLE OF CONTENTS.	vii
FIGURES.	ix
TABLES	xiii
INTRODUCTION	1
CONCLUSIONS AND RECOMMENDATIONS.	3
PROCEDURE.	5
SAMPLE COLLECTION	5
SAMPLE PREPARATION AND CHARACTERIZATION	5
PREPARATION OF SIMULATED LUNG FLUID	6
DISSOLUTION TECHNIQUES.	7
URANIUM ANALYSIS.	10
EVALUATION OF DISSOLUTION HALF-TIMES.	16
RESULTS.	16
CHARACTERIZATION OF SAMPLES	16
DISSOLUTION BEHAVIOR OF SAMPLES	18
SOLUBILITY CLASSIFICATIONS OF SAMPLES	51
DISCUSSION	52
COMPARISON OF CLASSIFICATIONS WITH LITERATURE VALUES.	53
COMPARISON OF PLANT-SAMPLE CLASSIFICATIONS WITH EXPECTATIONS.	54
REFERENCES	57
ACKNOWLEDGMENTS.	59

FIGURES

1. Schematic Production Lines for LWR-Fuel Rods.	4
2. Sample Container for Dissolution by the Sandwich Technique.	9
3. Sample Container for Dissolution by the Mini-Batch Technique.	11
4. Calibration Curve for Uranium Assay in Simulated Lung Fluid	12
5. Calibration Curve for Uranium Assay in Oxidized Simulated Lung Fluid at 425 nm	14
6. Calibration Curve for Uranium Assay as the Dibenzoylmethane Complex at 415 nm	15
7. Dissolution of Uranium Dioxide Dust, Obtained from the New Brunswick Laboratory, into Simulated Lung Fluid at 37°C	19
8. Dissolution of Uranium Octoxide Dust, Obtained from the New Brunswick Laboratory, into Simulated Lung Fluid at 37°C	20
9. Dissolution of Uranium Trioxide Dust Obtained from the New Brunswick Laboratory into Simulated Lung Fluid at 37°C.	21
10. Dissolution of Uranium Tetrafluoride Dust Obtained from the New Brunswick Laboratory into Simulated Lung Fluid at 37°C.	22
11. Dissolution of Ammonium Diuranate Dust Obtained from the Westinghouse Corporation into Simulated Lung Fluid at 37°C.	23
12. Dissolution of Dust Collected at Exxon's ADU Granulator Discharge into Simulated Lung Fluid at 37°C	24
13. Dissolution of Dust Collected at Exxon's ADU Calciner Discharge into Simulated Lung Fluid at 37°C	25
14. Dissolution of Dust Collected at Exxon's Pellet Grinder into Simulated Lung Fluid at 37°C	26
15. Dissolution of Dust Collected at Exxon's Scrap Recovery Area, into Simulated Lung Fluid at 37°C	27
16. Dissolution of Dust, Collected at Babcock & Wilcox's UF ₆ Hydrolyzer, into Simulated Lung Fluid at 37°C	28
17. Dissolution of Dust, Collected at Babcock & Wilcox's ADU Granulator Discharge, into Simulated Lung Fluid at 37°C	29
18. Dissolution of Dust, Collected at Babcock & Wilcox's ADU Calciner Discharge, into Simulated Lung Fluid at 37°C	30
19. Dissolution of Dust, Collected at Babcock & Wilcox's Reduction Kiln Discharge, into Simulated Lung Fluid at 37°C	31

FIGURES (cont'd)

20.	Dissolution of Dust, Collected at Babcock & Wilcox's Pellet Grinders, into Simulated Lung Fluid at 37°C	32
21.	Dissolution of Dust Collected at Babcock & Wilcox's Uranium Scrap Recovery Area, into Simulated Lung Fluid at 37°C	33
22.	Dissolution of Dust Collected at Babcock & Wilcox's Uranium Scrap Dissolver, into Simulated Lung Fluid at 37°C	34
23.	Dissolution of Dust Collected at Westinghouse's ADU Granulator Discharge, into Simulated Lung Fluid at 37°C	35
24.	Dissolution of Dust Collected at Westinghouse's Sintering Furnace Feed, into Simulated Lung Fluid at 37°C	36
25.	Dissolution of Dust Collected at Westinghouse's Uranium Scrap Recovery Area, into Simulated Lung Fluid at 37°C	37
26.	Dissolution of Dust Collected at General Electric's UF ₆ Vaporization Room, into Simulated Lung Fluid at 37°C	38
27.	Dissolution of Dust, Collected at General Electric's UF ₆ Hydrolyzer, into Simulated Lung Fluid at 37°C	39
28.	Dissolution of Dust, Collected at General Electric's ADU Calciner Feed, into Simulated Lung Fluid at 37°C	40
29.	Dissolution of Dust, Collected at General Electric's GECO Calciner Feed, into Simulated Lung Fluid at 37°C	41
30.	Dissolution of Dust Collected at General Electric's ADU Calciner Discharge, into Simulated Lung Fluid at 37°C	42
31.	Dissolution of Dust Collected at General Electric's GECO Calciner Discharge, into Simulated Lung Fluid at 37°C	43
32.	Dissolution of Dust Collected at General Electric's Pellet Press, into Simulated Lung Fluid at 37°C	44
33.	Dissolution of Dust Collected at General Electric's Pellet Grinder, into Simulated Lung Fluid at 37°C	45
34.	Dissolution of Dust Collected at General Electric's Chem Room Air Recirculation Intake, ADU End, into Simulated Lung Fluid at 37°C	46

FIGURES (cont'd)

35.	Dissolution of Dust Collected at General Electric's Chem Room Air Recirculation Intake, Center, into Simulated Lung Fluid at 37°C	47
36.	Dissolution of Dust Collected at General Electric's Chem Room Air Recirculation Intake, GECO End, into Simulated Lung Fluid at 37°C	48
37.	Optical Absorption Spectrum of 1.78 g/l Uranium Solution in Simulated Lung Fluid	49

TABLES

1. Compositions of Actual and Simulated Lung Fluids	7
2. Description of Samples	17
3. Microprobe and X-ray Crystallographic Analyses of Individual Particles	18
4. Weight Fractions and Dissolution Half-Times of Uranium Components	50
5. Dissolution-rate Classifications of Samples in Terms of the ICRP Task Group Lung Model	51

INTRODUCTION

The purpose of this study was to obtain airborne dust samples at various locations within plants manufacturing fuel elements for light-water reactors (LWR), and to classify the uranium-dissolution rates of these samples in terms of the ICRP Task Group Lung Model.¹ The International Commission on Radiological Protection developed this model for use in computing the radiation dose from radionuclides deposited in the lung. A key parameter is the classification of the deposited material according to the rate at which it leaves the lung. Three classes were established: D, W, and Y, corresponding to half-times in the lung of 0 to 10 days, 11 to 100 days, and >100 days, respectively. If clearance of the material from the lung is not strictly exponential with time, it is approximated by a sum of exponentials; and the material is classified according to the fractions of D, W, and Y components. In the absence of biological data, lung-clearance half-times for materials have been approximated by their dissolution half-times in simulated lung fluids.^{1,3} Although endocytosis and ciliary-mucus transport are known to contribute to lung clearance, experiments have indicated that a few days after dust deposition, dissolution determines the clearance rate for the lower respiratory tract.^{4,5} Given the lung-clearance classification for a material, its transport rates between other anatomical compartments are automatically assigned in the model. From these parameters, one can compute the residence times of the material and the associated radiation dose in each compartment.⁶

In the present study, uranium-bearing dust samples were obtained from four plants manufacturing LWR fuel elements. These plants were:

Babcock and Wilcox Co., Nuclear Materials Division,
Apollo, PA 15613

Exxon Nuclear Co., Richland, WA 99352

General Electric Co., Nuclear Energy Products Division,
Wilmington, NC 28401

Westinghouse Corp., Nuclear Fuel Division, Columbia, SC
29205

All four plants prepare fuel pellets by means of the ADU process, i.e., the conversion of uranium hexafluoride to ammonium diuranate (ADU) followed by its conversion to sintered uranium dioxide in pellet form according to the following steps:

Steps	Plant Area
1. $UF_6 \xrightarrow{H_2O} UO_2F_2$	UF_6 hydrolyzer
2. $UO_2F_2 \xrightarrow{NH_3} (NH_4)_2U_2O_7$	ADU precipitator
3. $(NH_4)_2U_2O_7 \xrightarrow{heat} (NH_4)_2U_2O_7 + UO_3$	ADU granulator
4. $(NH_4)_2U_2O_7, UO_3 \xrightarrow{heat} U_3O_8$	ADU calciner
5. $U_3O_8 \xrightarrow{H_2} UO_2$ (unsintered)	Reduction kiln
6. UO_2 (unsintered) $\xrightarrow{pressure}$ UO_2 (unsintered)	Pellet press
7. UO_2 (unsintered) \xrightarrow{heat} UO_2 (sintered)	Sintering furnace
8. UO_2 (sintered) $\xrightarrow{grinder}$ UO_2 (sintered)	Pellet grinder

Any uranium scrap produced in the above steps is reprocessed as follows:

8. U scrap $\xrightarrow{heat} U_3O_8$	Scrap furnace
9. $U_3O_8 \xrightarrow{HNO_3} UO_2(NO_3)_2$	Scrap dissolver

The General Electric Co. also produces fuel pellets in its plant by a "dry process," termed the GECO process. Here, the first four steps of the ADU process are replaced by the following two steps:

Step	Plant Area
1. $UF_6 \xrightarrow{dry\ steam} UO_2F_2 + U_3O_8 + UF_4$	GECO UF_6 converter
2. $UO_2F_2, U_3O_8, UF_4 \xrightarrow{H_2} UO_2$ (unsintered)	GECO calciner

The rest of the procedure is identical with the ADU process.

Since airborne dust formed in one area of a plant may be carried by convection or diffusion to other areas, it is important to consider the relative locations of the production equipment within a plant building.

Generally, several production lines are located in parallel, running from one end of the building to the other as shown schematically in Figure 1. It was expected that at least some of the dust samples would contain material from more than one source. For this reason, pure samples of UO_2 , U_3O_8 , UO_3 , UF_4 , and $(NH_4)_2U_2O_7$ were obtained and used for comparative dissolution measurements.

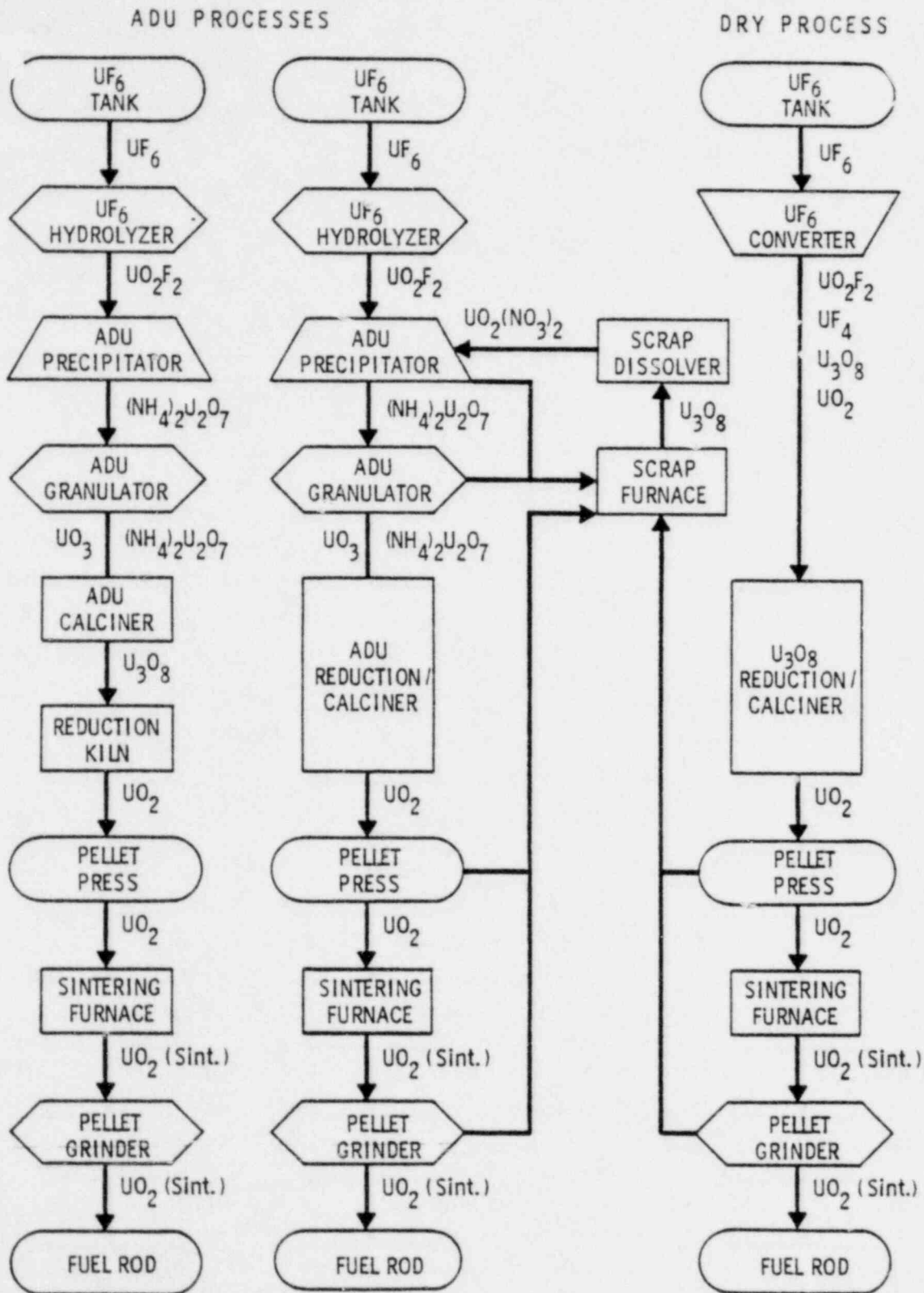
Dissolution-rate classifications were based on measurements of the fraction of uranium remaining undissolved in a sample as a function of time in simulated lung fluid at $37^\circ C$. Maximum dissolution rates were sought by means of rapid agitation of the samples because the lung is expected to be a site for efficient dissolution and because the values were to approximate clearance rates that include contributions from endocytosis and ciliary-mucus transport.

CONCLUSIONS AND RECOMMENDATIONS

Measurements of the fraction, F , of uranium remaining undissolved in a sample as a function of time in simulated lung fluid at $37^\circ C$ and expression of these data as a sum of exponential terms, $F = \sum_i f_i \exp(-0.693 t/T_i)$, provided a practical basis for classifying the sample's dissolution rate in terms of the ICRP Task Group Lung Model. In such an expression, f_i is the initial weight fraction of uranium component i with dissolution half-time T_i . Based on such measurements, the following classifications are recommended for pure uranium compounds expected as dust components in LWR-fuel plants: $(NH_4)_2U_2O_7$ - D; UO_3 - 48% D, 52% Y; UF_4 - Y; U_3O_8 - Y; and UO_2 - Y. The dissolution-rate classifications of the plant samples generally were in agreement with expectations based on process chemistry at a sample-collection site, the classifications for pure compounds listed above, and the generally accepted D classification for UF_6 , UO_2F_2 , and $UO_2(NO_3)_2$.

At the front end of the ADU and dry processes, the dust was found to be largely (46 to 96%) class D in uranium with some W and Y components depending upon the particular sampling location. One of three samples showed a large amount of Y component (17% D, 83% Y), and this unexpected result probably indicates that some air-sampling stations are exposed to unforeseen dust currents. At the ADU granulators and front ends of the ADU calciners, the dust was also found to be largely (45 to 72%) class D, with

FIGURE 1. Schematic Production Lines for LWR-Fuel Rods



the remainder being class Y. At the front ends of the dry-process calciners, the dust was found to dissolve somewhat less rapidly, indicating a classification of 34% D, 66% Y. From the discharge ends of the calciners to the grinders for the sintered fuel pellets, measurements showed that the dust should be classified 93 to 100% Y. The dissolution behavior of dust from the scrap-recovery areas indicated classifications ranging from 91% D, 9% W, to 100% Y, suggesting variable fractions of $UO_2(NO_3)_2$ and U_3O_8 in the samples. Thus, the dissolution-rate classification of uranium from dust varies substantially with location within a plant. The dissolution behavior of dust collected at the air-recirculation intakes for a room provides a composite classification of the dust generated therein, but individual workers in the room may be exposed to dust with a substantially different classification.

Concerning the mechanism of uranium dissolution in simulated lung fluid, it was concluded that uranium-bearing components in dust samples react with bicarbonate ion to form the soluble $[UO_2(CO_3)_3]^{4-}$ anion.

PROCEDURE

SAMPLE COLLECTION

Several dust samples were collected within each plant at locations determined by mutual consent of the staff health physicist and the author, following a tour of the facilities. The samples were collected by plant personnel close to the dust-generation sites within a given area. Generally, the samples were collected by drawing ambient air through cellulose or glass-fiber filters; but in a few cases, the samples consisted of dust which settled on metal dishes placed in the area.

Pure samples of UO_2 , U_3O_8 , UO_3 , and UF_4 were obtained from the New Brunswick Laboratory of the U. S. Department of Energy, Argonne, Illinois. A pure sample of ammonium diuranate was obtained from the Westinghouse Corporation, Nuclear Fuel Division, Columbia, South Carolina.

SAMPLE PREPARATION AND CHARACTERIZATION

Samples received on filters were dried in a desiccator over anhydrous calcium sulfate (J. T. Baker, Drierite) for two or three days, and then the

dust was "vacuumed off" the surface with a vacuum line fitted with a 25-mm diameter membrane filter (Millipore, Type HA in a Swinnex holder). The dust collected on the membrane filter was transferred into a glass vial with a camel-hair brush. Settled dust samples were also dried before being stored in glass vials.

The plant samples were generally too small for measurements of their specific surface areas, and the particle-size ranges could only be estimated by microscopic sizing. The particle-size ranges of the pure reference compounds were adjusted to the range 0 to 45 μm by sieving.

Some of the individual dust particles were analyzed with a microprobe analyzer to determine their uranium content and with an X-ray diffraction camera to determine their crystallographic forms. Unfortunately, it was not possible to develop precise methods for assaying a dust sample with respect to component compounds and their crystallographic forms, within the scope of the present study.

PREPARATION OF SIMULATED LUNG FLUID

The electrolyte compositions of human interstitial lung fluid and the simulant used in this study are shown in Table 1. Comparison shows that they are almost identical. The protein components of actual lung fluid were represented by an ionically equivalent amount of citrate in the simulant as suggested by Moss.⁸ Lung-fluid proteins are poorly characterized and generally not available in large quantities, and substitute proteins hinder filtration and promote bacterial growth in solutions. Phospholipids, also known to be present in trace amounts in actual lung fluid, were not included in the simulant for the same reasons. In a recent test,⁹ one of the suspected phospholipids, dipalmitoyl lecithin, was added to the simulant used in this experiment to form a 200 mg/l solution. No effect of this ingredient on the dissolution rate of uranium yellow cake samples was observed.

TABLE 1. Compositions of Actual and Simulated Lung Fluids

Ion	Actual ⁷	Simulated ⁸
Calcium, Ca ²⁺	5.0 meq/l	5.0 meq/l
Magnesium, Mg ²⁺	2.0 "	2.0 "
Potassium, K ⁺	4.0 "	4.0 "
Sodium, Na ⁺	145.0 "	145.0 "
Total Cations	156.0 "	156.0 "
Bicarbonate, HCO ₃ ⁻	31.0 meq/l	31.0 meq/l
Chloride, Cl ⁻	114.0 "	114.0 "
Citrate, H ₅ C ₆ O ₇ ³⁻	--	1.0 "
Acetate, H ₃ C ₂ O ₂ ⁻	7.0 "	7.0 "
Phosphate, HPO ₄ ²⁻	2.0 "	2.0 "
Sulfate, SO ₄ ²⁻	1.0 "	1.0 "
Protein	1.0 "	---
Total Anions	156.0 "	156.0 "
pH	7.3-7.4	7.3-7.4

Simulated lung fluid with the composition shown in Table 1 was prepared by slowly adding the following ingredients in order to 990 ml of distilled water and adjusting the final volume to 1000 ml:

0.2033 g MgCl₂·6H₂O
 6.0193 g NaCl
 0.2982 g KCl
 0.2680 g Na₂HPO₄·7H₂O
 0.0710 g Na₂SO₄
 0.3676 g CaCl₂·2H₂O
 0.9526 g NaH₃C₂O₂·3H₂O
 2.6043 g NaHCO₃
 0.0970 g Na₃H₃C₆O₇·2H₂O

If the pH of the resulting solution was not 7.3-7.4, it was adjusted to this value with small volumes of 1 N HCl.

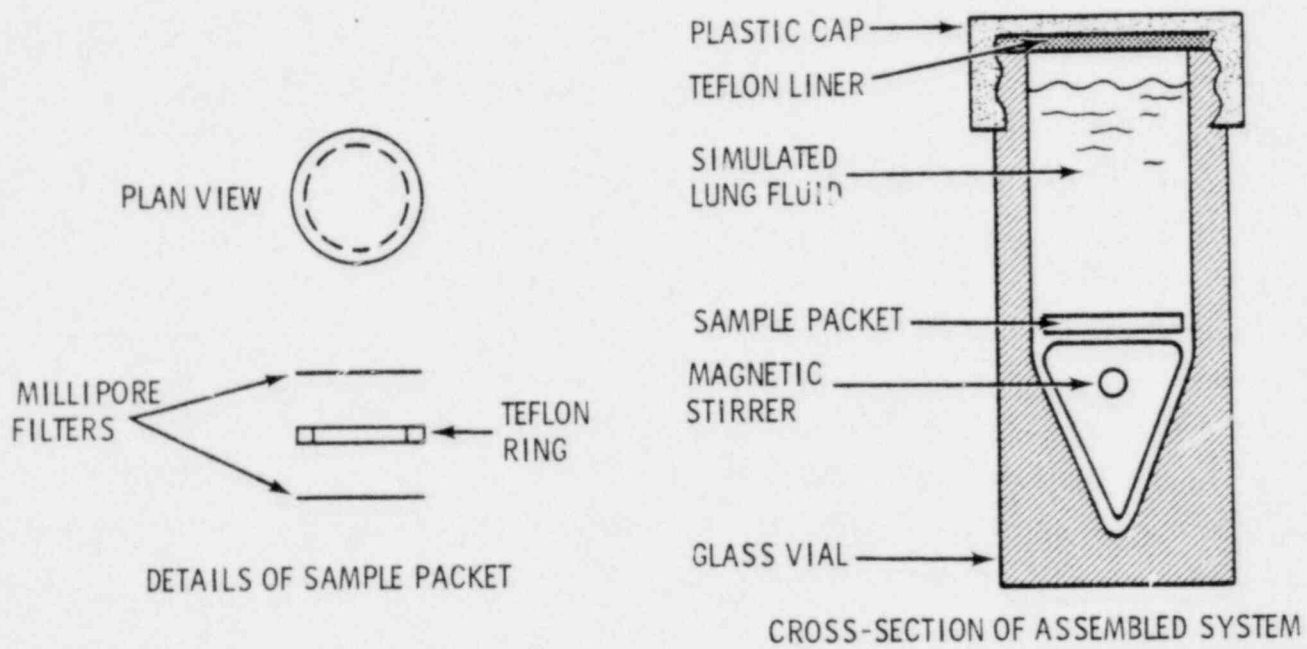
DISSOLUTION TECHNIQUES

Dissolution trials on the uranium dust samples were conducted in well-agitated portions of simulated lung fluid (SLF) at 37°C. Depending on the amount of sample available, one of three dissolution techniques was used.

The "batch" technique described recently¹⁰ was used when relatively large samples were available, such as those of the New Brunswick Laboratory reference compounds. A 0.6-g dust sample was added to a 125-ml Erlenmeyer flask together with 100 ml of SLF. The flask was then closed with a glass stopper and agitated in a shaker bath at $37\pm 1^\circ\text{C}$. After selected time periods, the flask was removed from the shaker, and the suspension was filtered through a membrane filter (Millipore, 45-mm diameter, HA, $0.45\ \mu\text{m}$ pore size). The filtrate was analyzed for uranium, and the undissolved dust was washed back into the Erlenmeyer flask with 100 ml of fresh SLF. The flask was then replaced in the shaker bath for an additional time period. The pH of the suspension was checked every three days and adjusted to 7.3-7.4 with dilute hydrochloric acid, if necessary. At the end of 60 days, the undissolved residue in the flask was dissolved in 5.00 ml of warm, concentrated nitric acid and analyzed for uranium.

A second dissolution technique, termed the "sandwich" technique, was designed for use with much smaller samples of uranium-bearing dust. A 0.05-g dust sample was sandwiched between two membrane filters (Millipore, 10-mm diameter, VF, $0.01\ \mu\text{m}$ pore size) separated by a Teflon ring, 12.5-mm O.D., 8.5 mm I.D. and 0.85-mm thick. Millipore Cement, Formulation No. 1, was used to bond the filters to the ring. Dissolution was started by dropping the sandwich into a 3-ml, conical-bottom vial (Pierce Chemical, Reacti-Vial) containing 3.00 ml of SLF and a Teflon-coated, magnetic stirrer as shown in Figure 2. The vial was closed with a Teflon-lined screw cap and placed in a heating block/stirrer assembly (Pierce Chemical, Reacti-Therm System) which drove the magnetic stirrer and kept the suspension within $37\pm 1^\circ\text{C}$. SLF permeated the sandwich and any soluble uranium rapidly diffused out into the well-stirred surrounding fluid. After selected time periods, the exposed SLF was removed from the vial for uranium analysis, and 3.00 ml of fresh SLF was added to the vial to continue the dissolution. The pH of the suspension was checked every three days and adjusted to 7.3-7.4 with dilute hydrochloric acid, if necessary. After 60 days, the undissolved sample in the sandwich was dissolved in 3.00 ml of warm concentrated nitric acid and analyzed for uranium. Although this technique was used successfully on the first few samples of fuel-plant dust, the sandwiches proved to be more fragile than

FIGURE 2. Sample Container for Dissolution by the Sandwich Technique



anticipated, requiring occasional repackaging of the sample. Thus, the technique described in the following paragraph was designed as an alternative.

A third dissolution technique, termed the "mini-batch" technique, was used with most of the samples of fuel-plant dust. Dissolution was started by adding a 0.05-g dust sample to a 5-ml, conical-bottom vial (Pierce Chemical, Reacti-Vial) containing 5.00 ml of SLF and a Teflon-lined magnetic stirrer as shown in Figure 3. The vial was closed with a Teflon-lined screw cap and kept at $37 \pm 1^\circ\text{C}$ in the same heating block/stirrer assembly as described in the preceding paragraph. After selected time periods, the vial was removed from the heating block and centrifuged to force the undissolved dust into the conical end. The cap was then opened, and the supernatant fluid was drawn through a stainless steel needle into a plastic syringe. A membrane filter (Millipore, 13-mm diameter, GC, $0.22 \mu\text{m}$ pore size) in a stainless steel filter holder (Millipore, Swinnex) was fitted on the end of the syringe, and the solution was filtered into a container and stored for uranium analysis. The membrane filter was then removed with stainless steel forceps, and 5.00 ml of fresh SLF was added to the barrel of the syringe. The filter holder, minus filter, and the syringe needle were refitted on the syringe; and the small amount of solid sample held on the filter was washed off into the vial with a jet of SLF from the syringe. The vial was then capped, vortexed to re-suspend all the remaining sample and replaced in the heating block. The pH of the suspension was checked every three days and adjusted to 7.3-7.4 with dilute HCl, if necessary. At the end of 60 days, the residual sample was dissolved in 5.00 ml of warm concentrated nitric acid and analyzed for uranium.

URANIUM ANALYSIS

The filtrates obtained in dissolution trials using the batch technique were analyzed for uranium in one of two ways. If the dissolved uranium was known to be in the hexavalent state, the absorbance of the filtrate was measured directly in a 1-dm spectrophotometer cell at 448 nm versus a solution of uranium-free simulated lung fluid. The calibration curve for this assay method, using standard solutions of uranium, is shown in Figure 4. The concentration of uranium in a filtrate was obtained by dividing the measured absorbance by 1.005, the absorptivity of the uranium in $\text{lg}^{-1}\text{dm}^{-1}$. If the

FIGURE 3. Sample Container for Dissolution by the Mini-Batch Technique

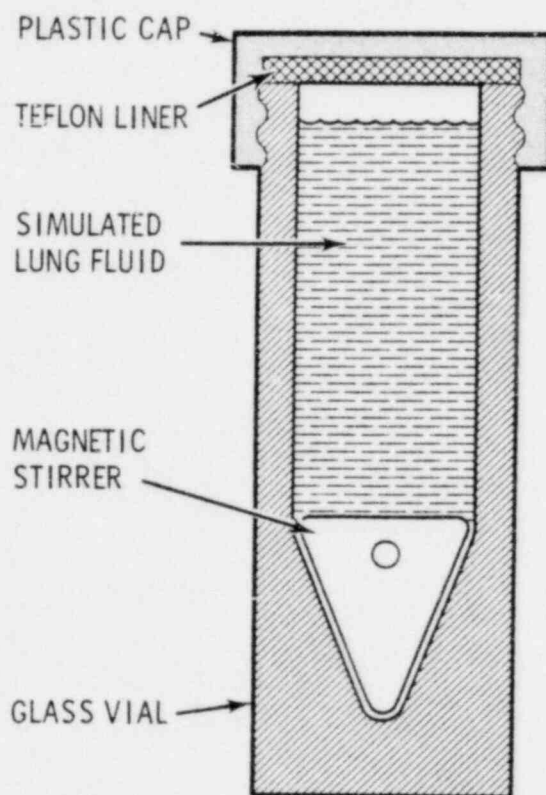
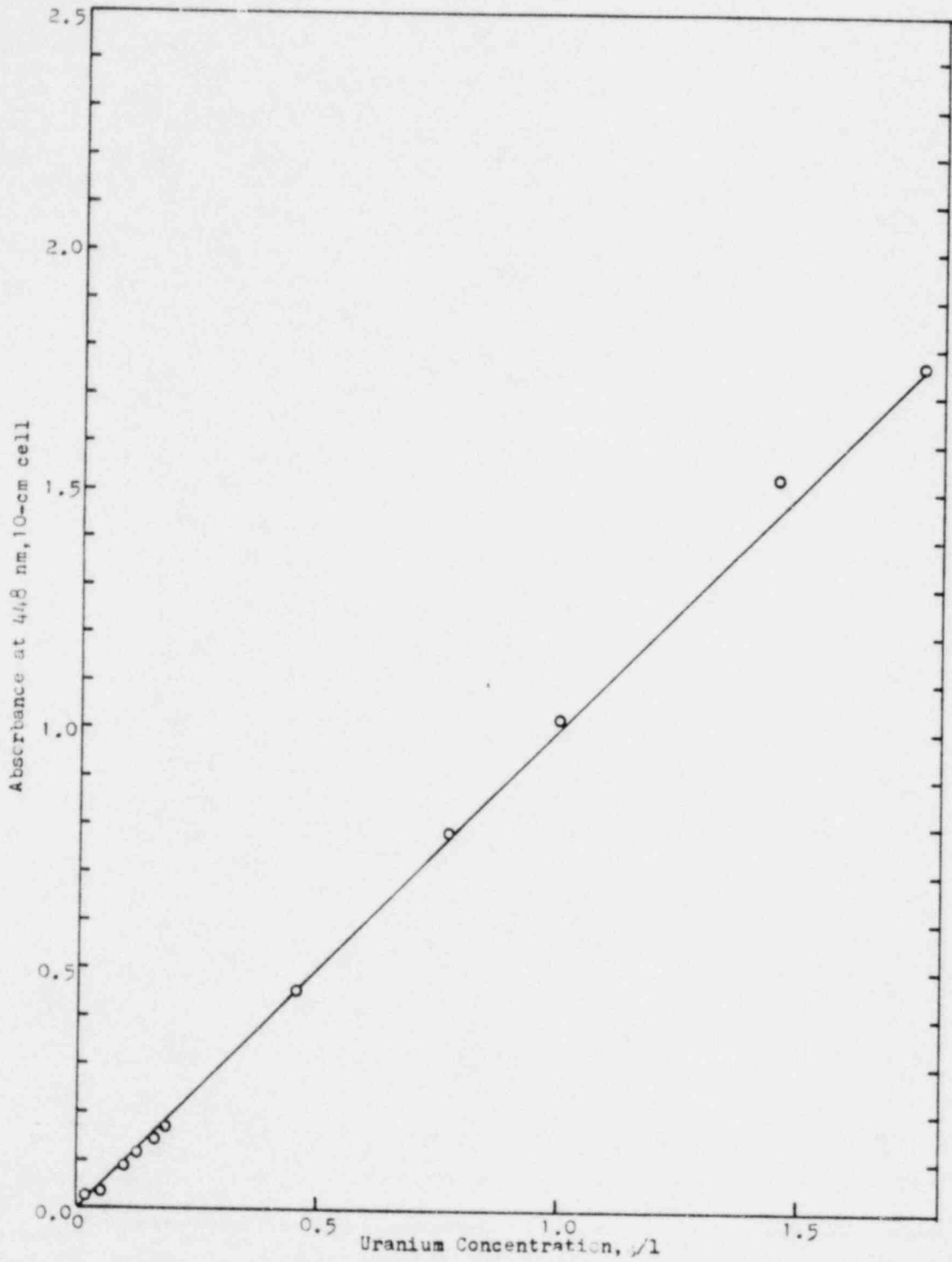


FIGURE 4. Calibration Curve for Uranium Assay in Simulated Lung Fluid at 448 nm



valence state of the dissolved uranium was uncertain, 3.0 g of periodic acid was dissolved in the 100-ml volume of filtrate, and the solution was heated to 80°C for one minute in order to convert all uranium to the hexavalent state. After this solution cooled to room temperature, its absorbance was measured in a 1-dm spectrophotometer cell at 425 nm versus a solution of similarly treated, uranium-free simulated lung fluid. The calibration curve for this assay is shown in Figure 5. The concentration of uranium in a filtrate was obtained by dividing its absorbance by 0.577, the absorptivity of uranium in $\text{lg}^{-1}\text{dm}^{-1}$.

The filtrates obtained in dissolution trials using the sandwich or mini-batch techniques were analyzed in two other ways. If the concentration of uranium exceeded 2×10^{-5} g/l, the filtrate was analyzed by the method of Mæeck, et al¹¹, as modified by Rodden.¹² Analysis consisted of acidifying 500 μl of filtrate with 500 μl of concentrated nitric acid in a 2-dram glass vial. A 0.004 N potassium permanganate solution was then added dropwise until the solution was pink in order to insure oxidation of any uranium to the hexavalent state. A drop of 0.04 N hydroxylamine hydrochloride was added subsequently to chemically reduce the excess permanganate. A 4.0-ml portion of 0.005 M tetrapropylammonium hydroxide/2.8 M aluminum nitrate (2.0 M acid deficient) solution¹² and 2.0 ml of hexone (methyl isobutyl ketone) were then added. The vial was closed with a plastic-lined screw cap and the contents were vigorously agitated on a vortex mixer to extract the tetrapropylammonium-uranium complex into the hexone phase. The hexone extract was transferred to a clean 2-dram vial and extracted with 5 ml of an aqueous scrub solution to remove any metals that would interfere with the uranium analysis. The scrub solution contained 2.5 M aluminum nitrate (1.0 M acid deficient), 0.22 M tartaric acid, 0.25 M oxalic acid, and 0.22 M ethylenediaminetetraacetic acid.¹¹ A 1.00-ml aliquot of the scrubbed hexone solution was added to 15.0 ml of 0.001 M dibenzoylmethane (Eastman No. 2197) in 95% pyridine/5% ethanol to form the colored uranium-dibenzoylmethane complex. This solution was transferred to a 5.00-cm spectrophotometer cell, and its absorbance at 415 nm was measured versus a solution prepared from uranium-free SLF by the same procedure. The absorbance increased linearly with uranium concentration as shown in Figure 6, and the absorptivity was found to be $667 \text{lg}^{-1}\text{dm}^{-1}$.

FIGURE 5. Calibration Curve for Uranium Assay in Oxidized Simulated Lung Fluid at 425 nm

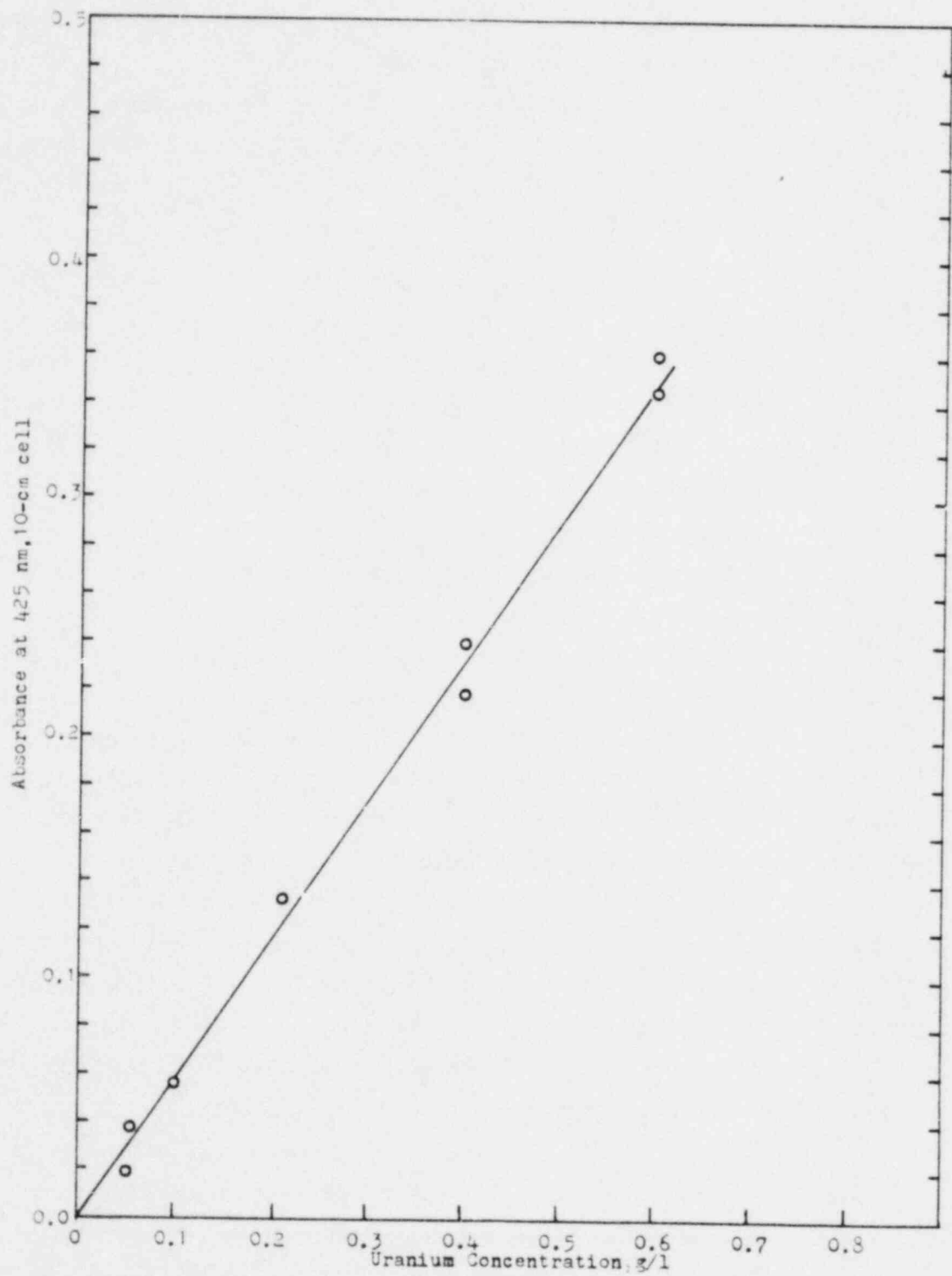
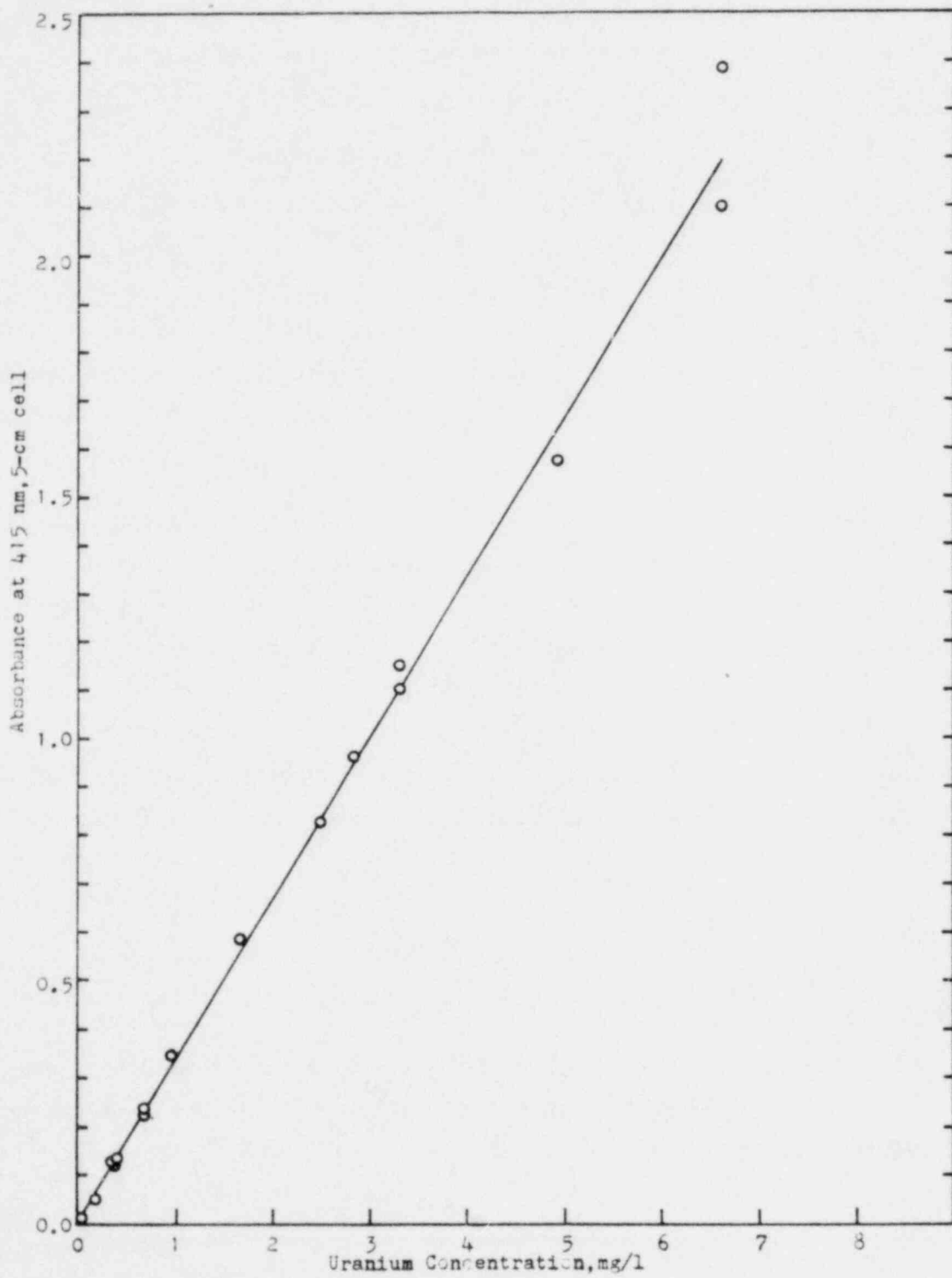


FIGURE 6. Calibration Curve for Uranium Assay as the Dibenzoylmethane Complex at 415 nm



The concentration of uranium in the original filtrate was obtained in g/l by multiplying the absorbance of the pyridine solution at 415 in a 5-cm cell by $16 \times 2 \times 2/667 \times 0.5 = 0.192$. Filtrates containing less than 2×10^{-5} g U/l were analyzed at the Hanford Engineering Development Laboratory of the Westinghouse Corporation by direct fluorometric analysis essentially as described in ASTM procedure D2907-75, method A.¹³ The sensitivity of this procedure was 1×10^{-6} g U/l.

EVALUATION OF DISSOLUTION HALF-TIMES

Dissolution theory indicates that the fraction of a pure sample remaining undissolved should decrease exponentially with time, unless the particle size range is very broad.¹⁴ Since the samples were expected to contain more than one uranium component with differing dissolution half-times, the data were expected to fit an equation of the form:

$$F = f_1 \exp(-0.693t/T_1) + f_2 \exp(-0.693t/T_2) + \dots + f_n \exp(-0.693t/T_n)$$

where F is the fraction of total uranium remaining undissolved after time t , and the f_i are the initial weight fractions of uranium components in the sample with dissolution half-times t_i . The values of F were calculated by subtracting the amount of uranium dissolved during any sampling period from the amount undissolved at the beginning of that period and dividing this quantity by the total amount of uranium in the sample. Preliminary values of f_i and T_i were obtained by graphical analysis of the data, and these were then used as starting values in an iterative computer program (Subroutine NREG from the Madison Academic Computing Center) to obtain the best fit to data by regression analysis.

RESULTS

CHARACTERIZATION OF SAMPLES

Dissolution trials were conducted on a total of 30 samples. These are listed in Table 2 together with their particle-size ranges, colors, and expected uranium components.

TABLE 2. Description of Samples

<u>Sample</u>	<u>Color</u>	<u>Size Range</u>	<u>Expected Components</u>
Ammonium diuranate	Yellow	0 - 45 μm	$(\text{NH}_4)_2\text{U}_2\text{O}_7$
Uranium trioxide	Yellow	0 - 45 μm	UO_3
Uranium octoxide	Greenish black	0 - 45 μm	U_3O_8
Uranium dioxide	Brownish black	0 - 45 μm	UO_2
Uranium tetrafluoride	Green	0 - 45 μm	UF_4
<u>Exxon Plant Dust</u>			
ADU granulator discharge	Yellow	0 - 40 μm	$(\text{NH}_4)_2\text{U}_2\text{O}_7$
ADU reduction kiln discharge	Brown	0 - 10 μm	UO_2
Pellet grinder	Brownish black	0 - 25 μm	UO_2 (sint.)
U scrap recovery area	Black	0 - 25 μm	U_3O_8
<u>Babcock and Wilcox Plant Dust</u>			
UF_6 hydrolyzer	Gray	0 - 50 μm	UO_2F_2
ADU granulator discharge	Yellow	0 - 25 μm	$(\text{NH}_4)_2\text{U}_2\text{O}_7$
ADU calciner discharge	Brown	0 - 25 μm	U_3O_8
U_3O_8 reduction kiln discharge	Brown	0 - 10 μm	UO_2
Pellet grinder	Brownish black	0 - 25 μm	UO_2 (sint.)
U scrap recovery area	Black	0 - 25 μm	$\text{UO}_2(\text{NO}_3)_2$, U_3O_8
U scrap dissolver	Yellow/black	0 - 25 μm	$\text{UO}_2(\text{NO}_3)_2$
<u>Westinghouse Plant Dust</u>			
ADU calciner feed	Yellow brown	0 - 10 μm	$(\text{NH}_4)_2\text{U}_2\text{O}_7$, U_3O_8
Sintering furnace discharge	Brownish black	0 - 10 μm	UO_2 (sint.)
U scrap recovery area	Gray	0 - 10 μm	$\text{UO}_2(\text{NO}_3)_2$, U_3O_8
<u>General Electric Dust</u>			
UF_6 vaporization room	Gray	0 - 50 μm	UF_6 , UO_2F_2
UF_6 vaporizer/dissolver	Light yellow	0 - 25 μm	UO_2F_2
ADU calciner feed	Yellow	0 - 10 μm	$(\text{NH}_4)_2\text{U}_2\text{O}_7$
GECO calciner feed	Brown	0 - 5 μm	UO_2F_2 , UF_4 , U_3O_8 , UO_2
ADU calciner discharge	Brown	0 - 50 μm	U_3O_8 , UO_2
GECO calciner discharge	Brown	0 - 50 μm	U_3O_8 , UO_2
Pellet presses	Brown	0 - 10 μm	UO_2
Pellet grinder	Brown	0 - 5 μm	UO_2
Chem. room air, ADU end	Light brown	0 - 50 μm	All of above
Chem. room air, center	Light brown	0 - 50 μm	All of above
Chem. room air, GECO end	Light brown	0 - 50 μm	All of above

Microprobe and X-ray crystallographic analyses of a randomly selected particle from three of the samples obtained from the Exxon Nuclear Co. are tabulated below.

TABLE 3. Microprobe and X-Ray Crystallographic Analyses of Individual Particles

<u>Sample</u>	<u>Microprobe Assay</u>	<u>Crystal Form</u>
ADu reduction kiln (Exxon)	83% U	Cubic UO ₂
Pellet grinder (Exxon)	85% U	Cubic UO ₂
U scrap recovery (Exxon)	77% U	Hexagonal U ₃ O ₈

DISSOLUTION BEHAVIOR OF SAMPLES

The dissolution behavior of the samples is shown graphically in Figures 7 to 36. Most of the graphs consist of a single curve; however, those for uranium trioxide (Figure 9) and ammonium diuranate (Figure 11) show multiple sets of data. In Figure 9, dissolution patterns obtained for UO₃ by both the batch and mini-batch techniques are compared and shown to be quite similar. In Figure 11, dissolution patterns for (NH₄)₂U₂O₇ by both the mini-batch and sandwich methods are compared and shown to be identical. Also shown in Figure 11 are dissolution patterns for portions of this sample by the batch method both 15 months earlier and 9 months later than this comparison. The steady increase in dissolution half-time suggests that chemical changes occurred in the sample during storage in air at 23°C. The uranium content of the sample was also found to increase from 74.6% in April, 1978 to 76.7% two years later.

The importance of bicarbonate ion in the dissolution of uranium is also shown in Figure 11, where the non-dissolution of (NH₄)₂U₂O₇ in bicarbonate-free SLF is depicted. Figure 37 shows the optical absorption spectrum of (NH₄)₂U₂O₇ dissolved in regular SLF, and it corresponds closely to published spectra of the $[UO_2(CO_3)_3]^{4-}$ anion.¹⁵ Similar spectra, differing only in absorption intensity, were obtained for all the samples that underwent appreciable dissolution.

The dissolution data were fitted into expressions of the form:

$$F = f_1 \exp(-0.693t/T_1) + f_2 \exp(-0.693t/T_2) - f_3 \exp(-0.693t/T_3) + \dots$$

FIGURE 7. Dissolution of Uranium Dioxide Dust, Obtained from the New Brunswick Laboratory, into Simulated Lung Fluid at 37°C

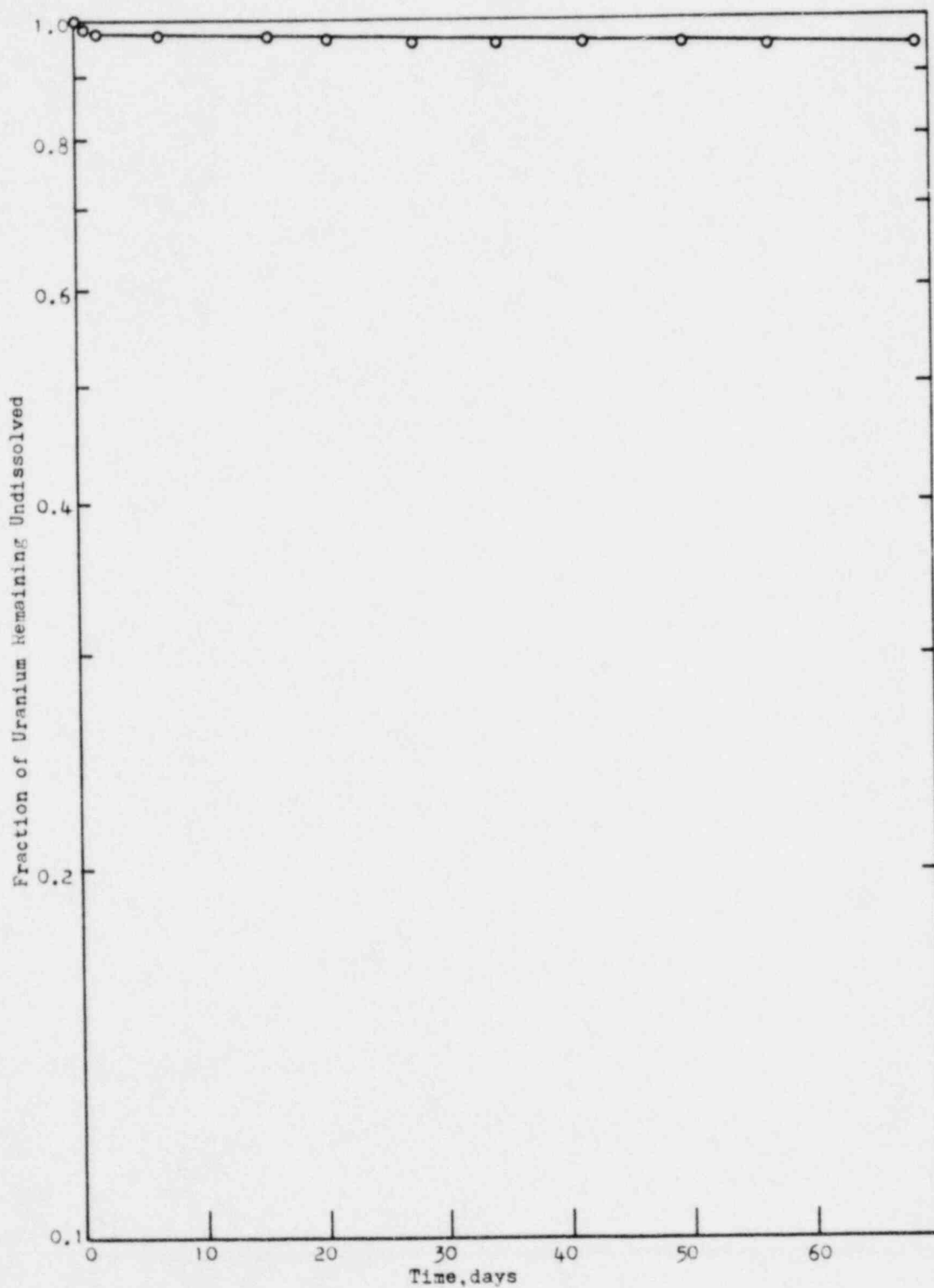


FIGURE 8. Dissolution of Uranium Octoxide Dust, Obtained from the New Brunswick Laboratory, into Simulated Lung Fluid at 37°C

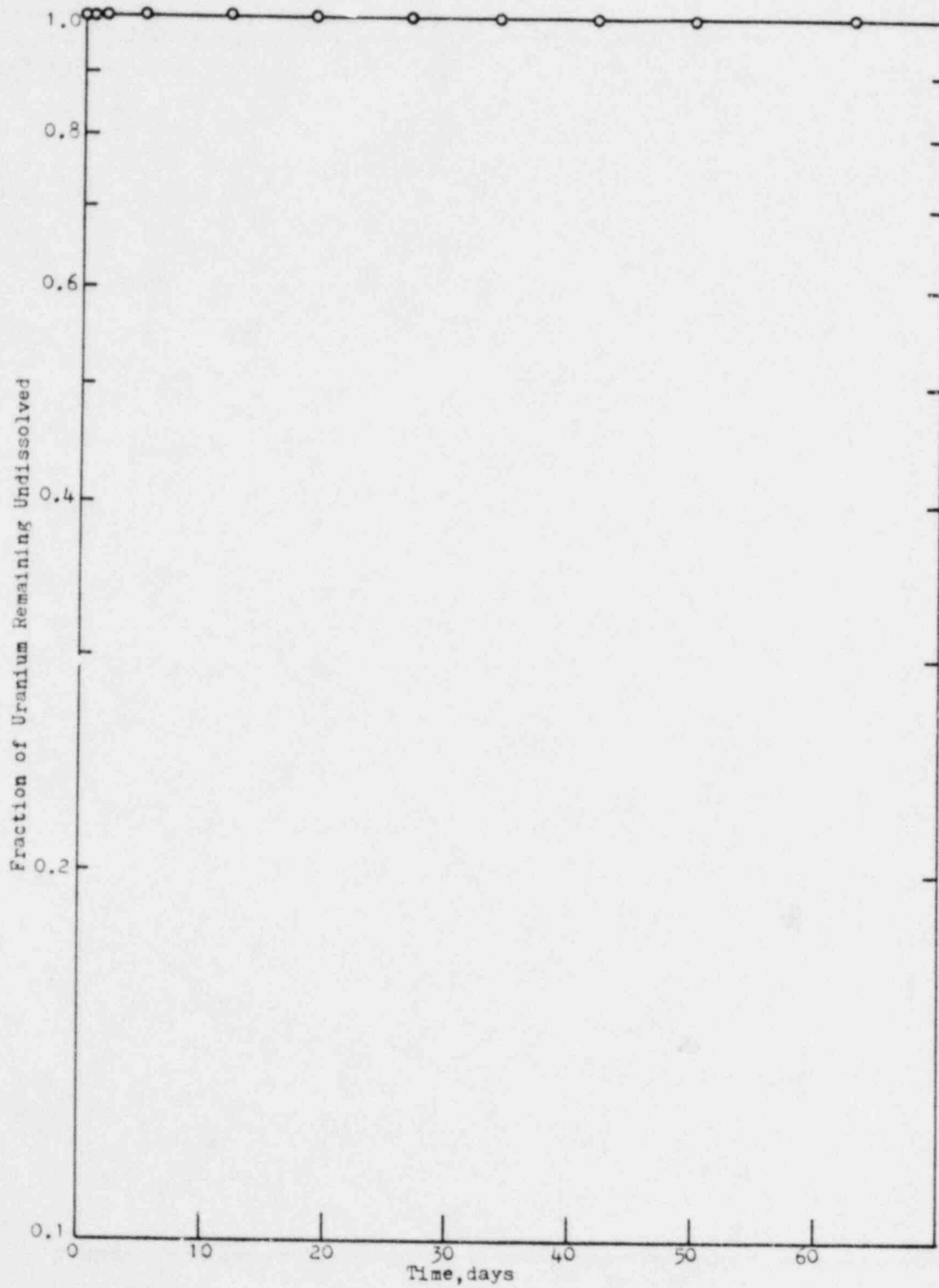


FIGURE 9 Dissolution of Uranium Trioxide Dust, Obtained from the New Brunswick Laboratory, into Simulated Lung Fluid at 37°C. (Data from batch method shown by open circles. Data from mini-batch method shown by closed circles.)

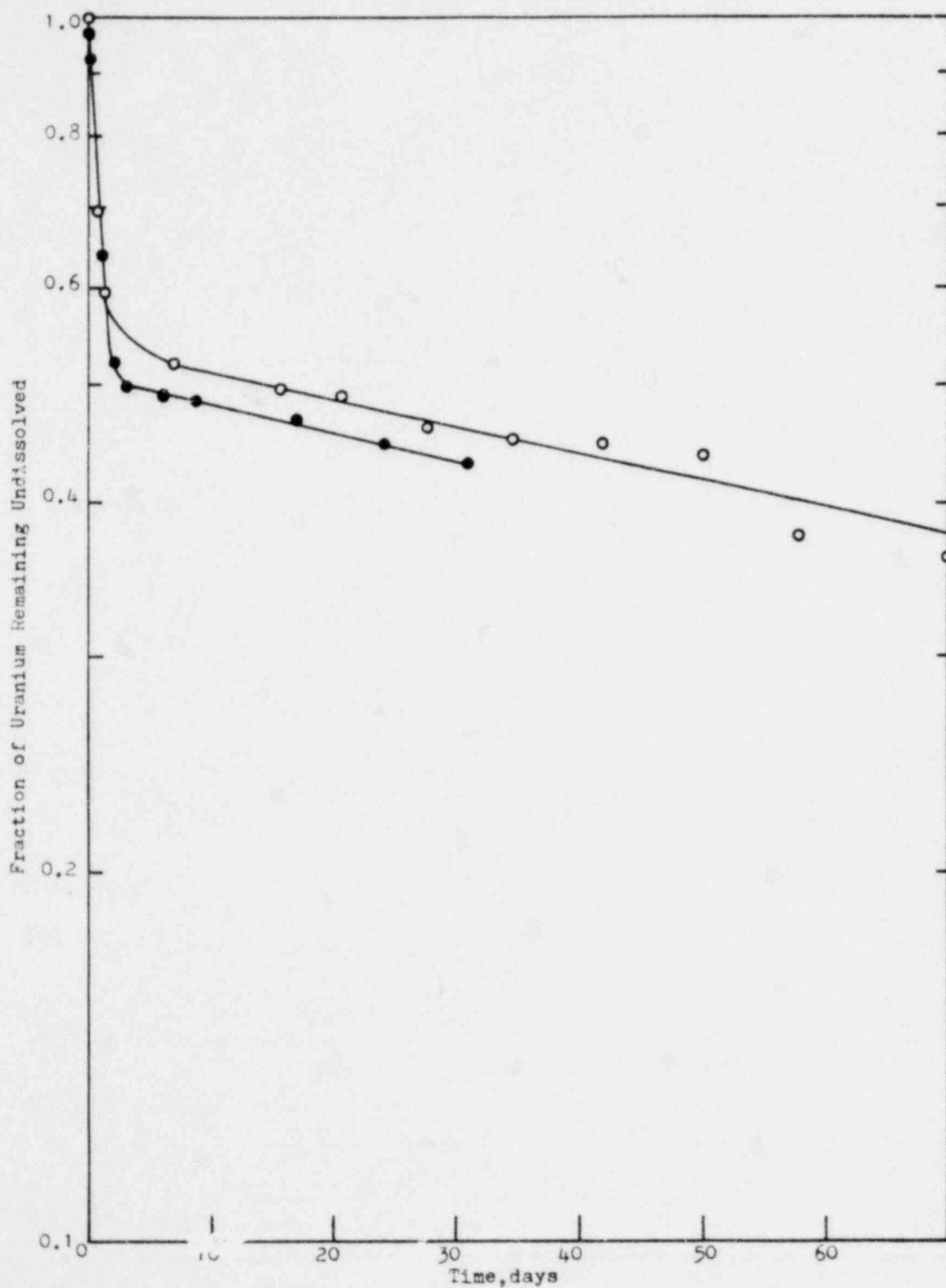


FIGURE 10. Dissolution of Uranium Tetrafluoride Dust, Obtained from the New Brunswick Laboratory, into Simulated Lung Fluid at 37°C

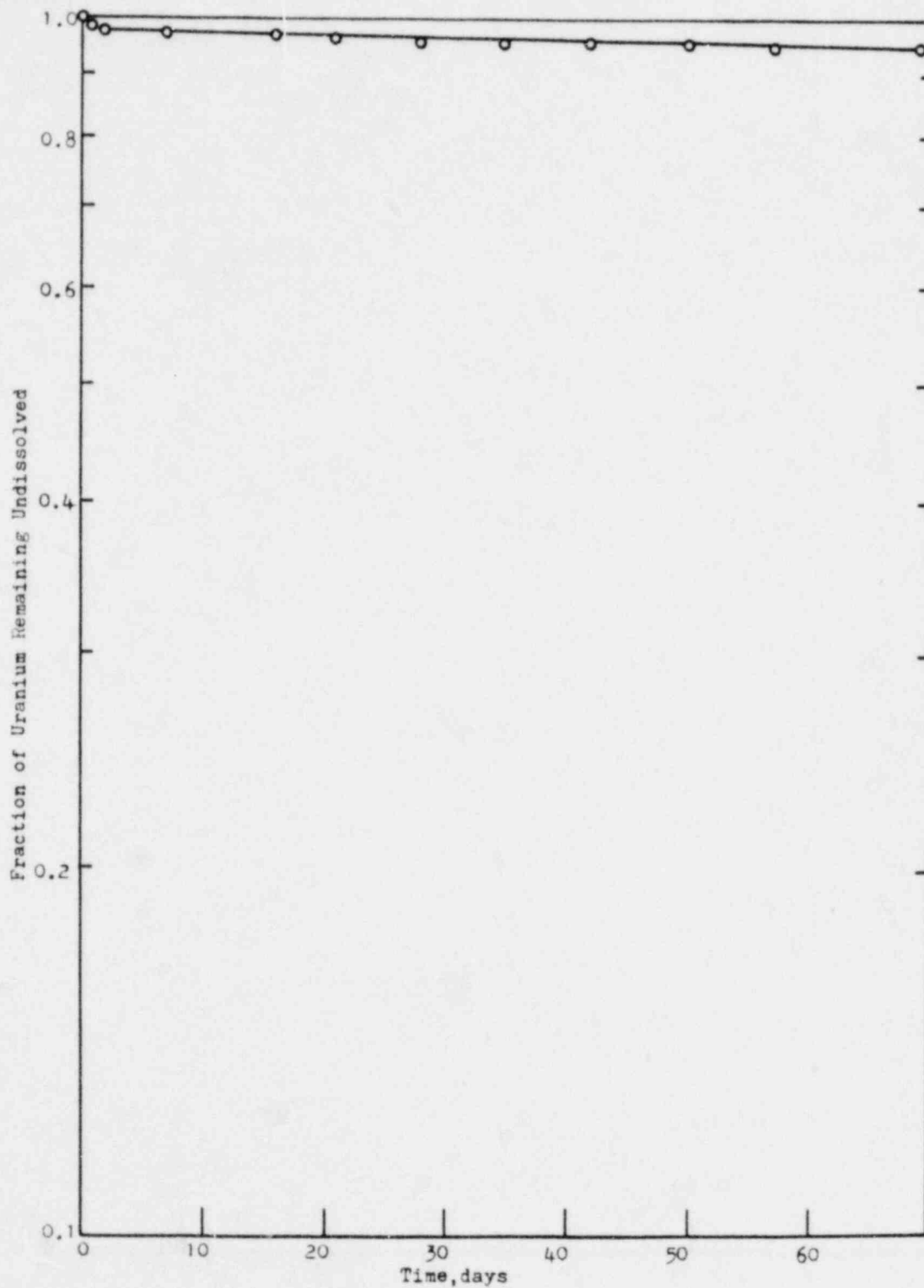


FIGURE 11. Dissolution of Ammonium Diuranate Dust, Obtained from the Westinghouse Corporation, into Simulated Lung Fluid at 37°C. Data from April 1978, batch method (o); July 1979, sandwich (Δ) and mini-batch (\blacktriangle) methods, and March 1980, batch method (\square). Dissolution into bicarbonate-free simulated lung fluid, mini-batch method (\blacksquare).

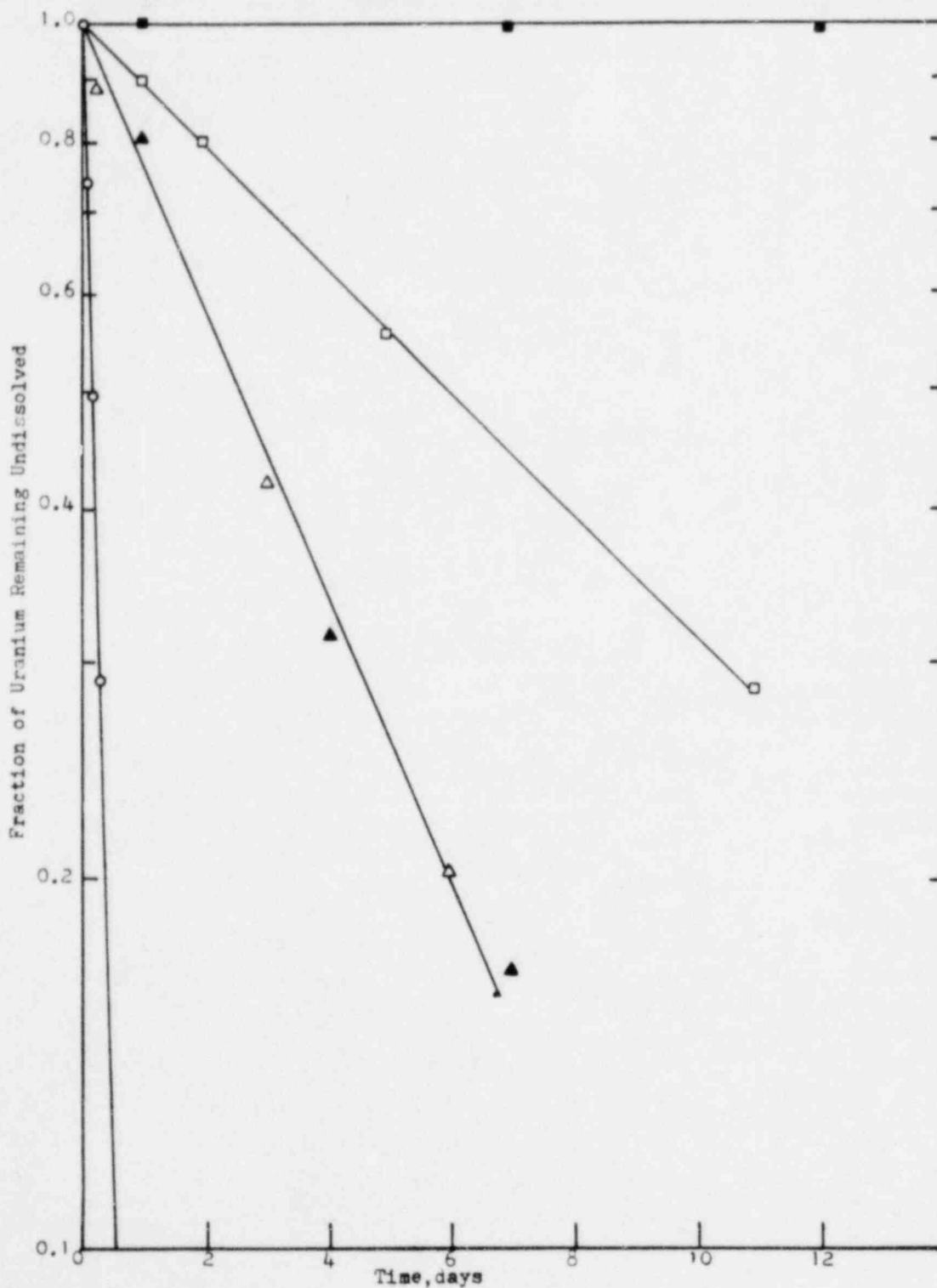


FIGURE 12. Dissolution of Dust, Collected at Exxon's ADU Granulator Discharge, into Simulated Lung Fluid at 37°C

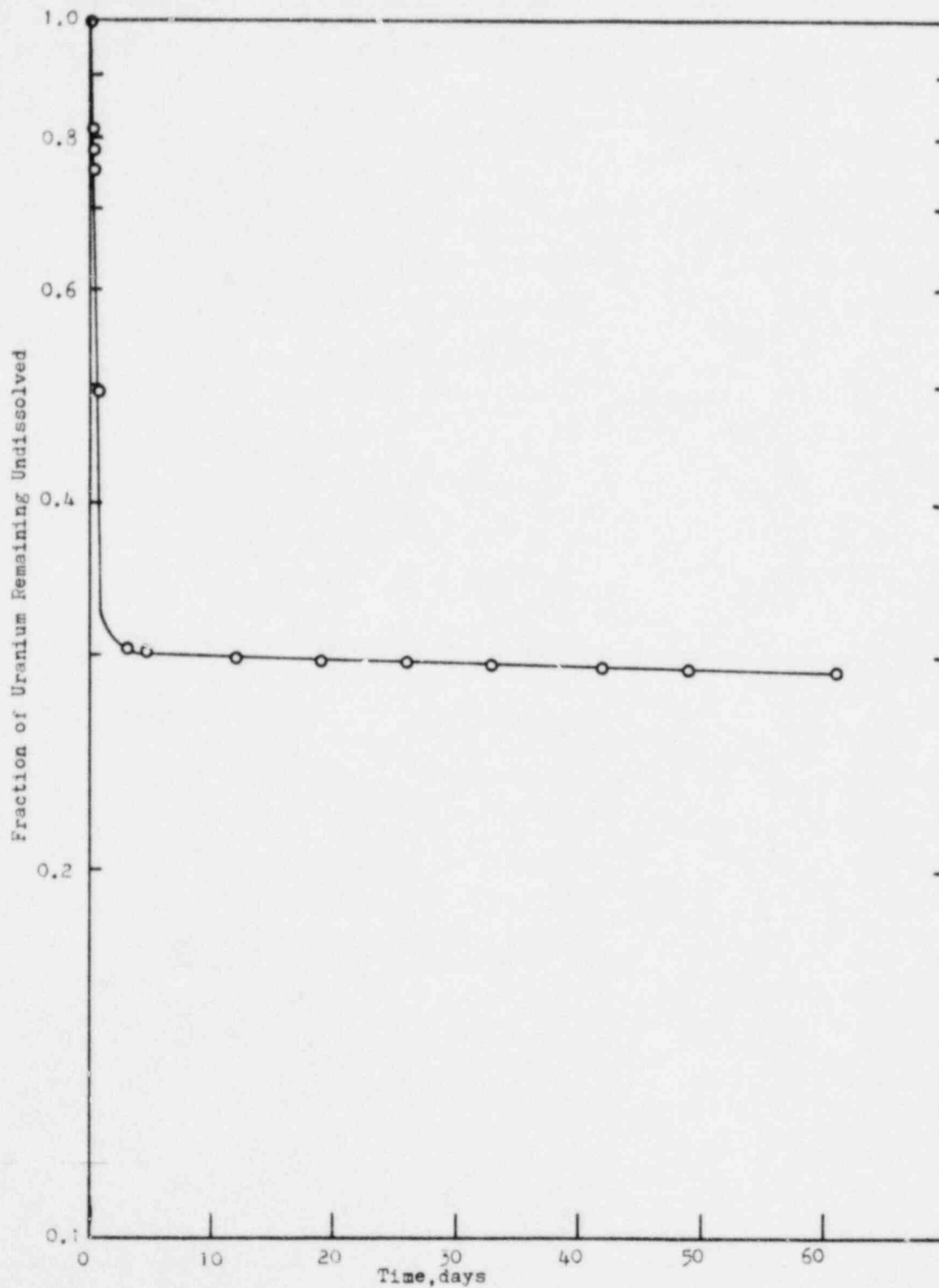


FIGURE 13. Dissolution of Dust, Collected at Exxon's ADU Calciner Discharge, into Simulated Lung Fluid at 37°C

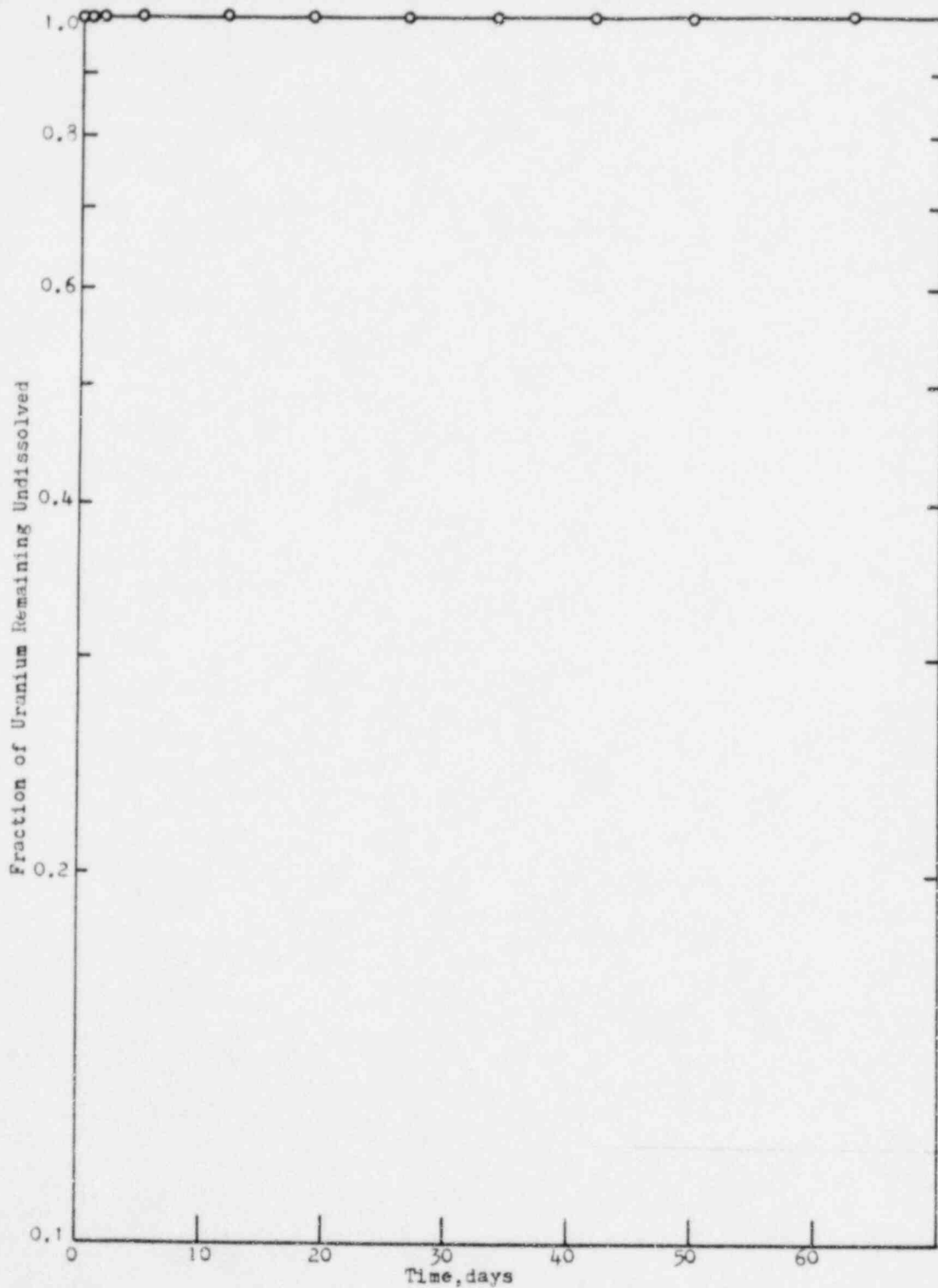


FIGURE 14. Dissolution of Dust, Collected at Exxon's Pellet Grinder, into Simulated Lung Fluid at 37°C

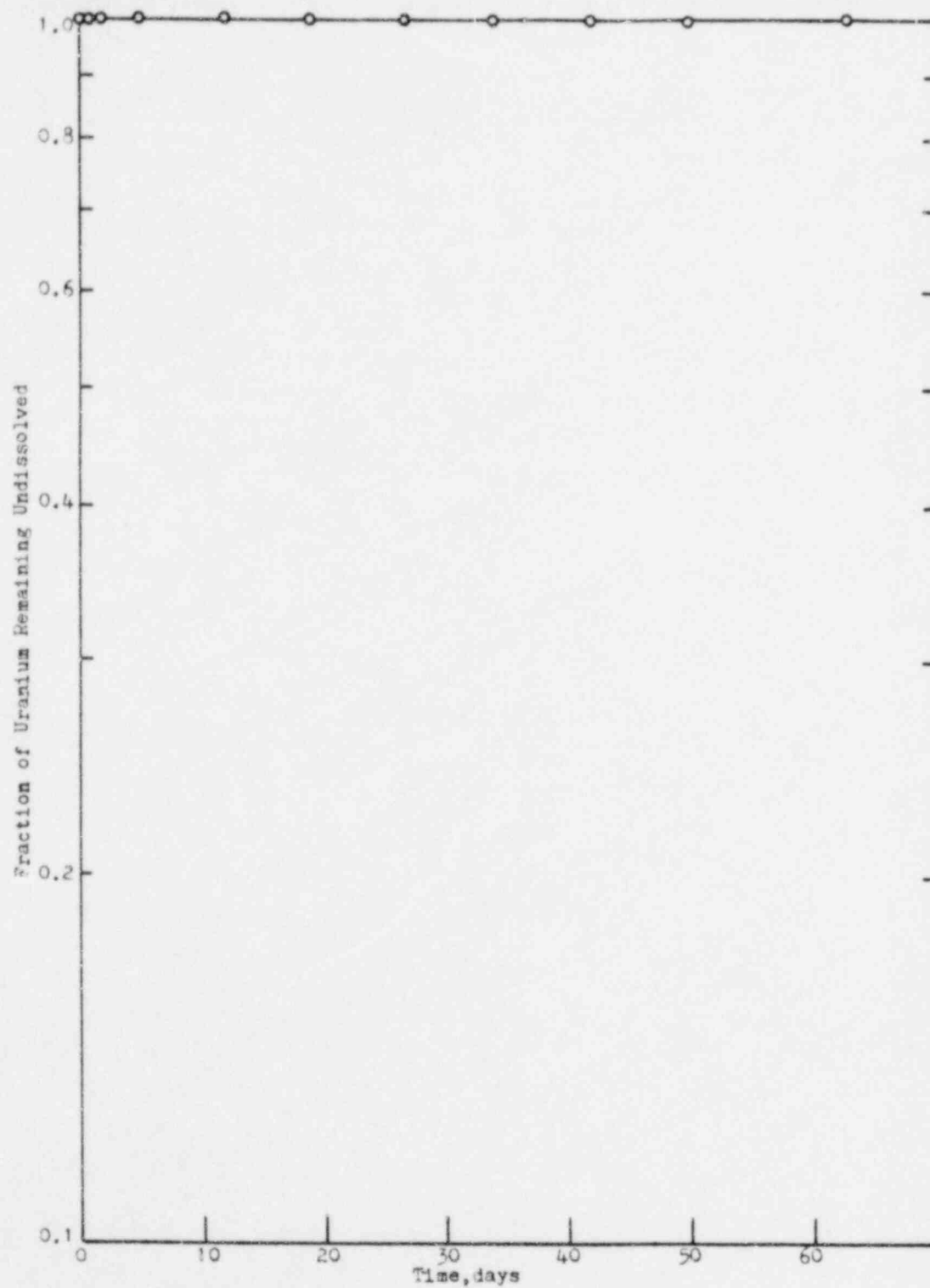


FIGURE 15. Dissolution of Dust, Collected at Exxon's Scrap Recovery Area, into Simulated Lung Fluid at 37°C

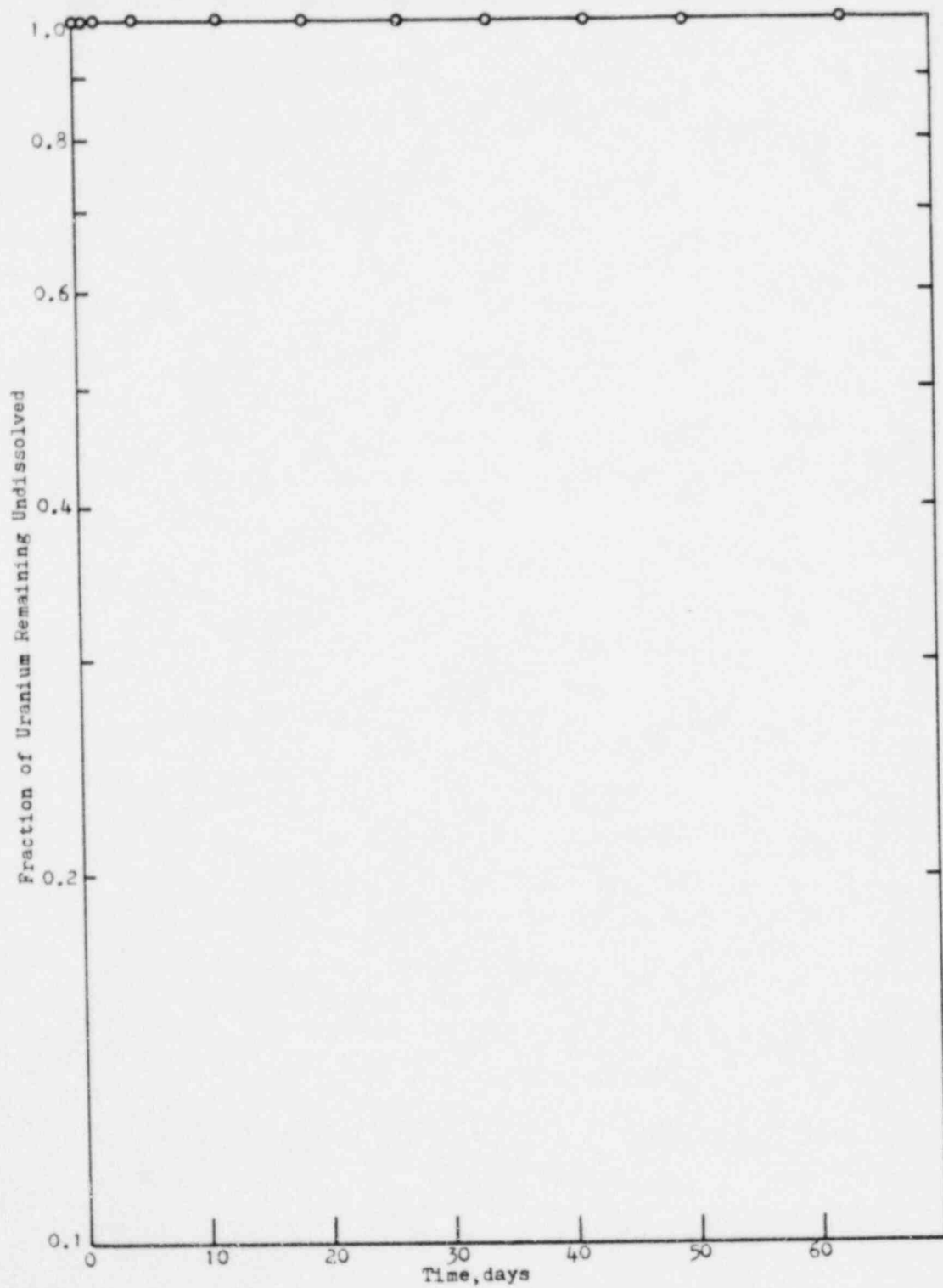


FIGURE 16. Dissolution of Dust, Collected at Babcock & Wilcox's UF_6 Hydrolyzer, into Simulated Lung Fluid at $37^\circ C$

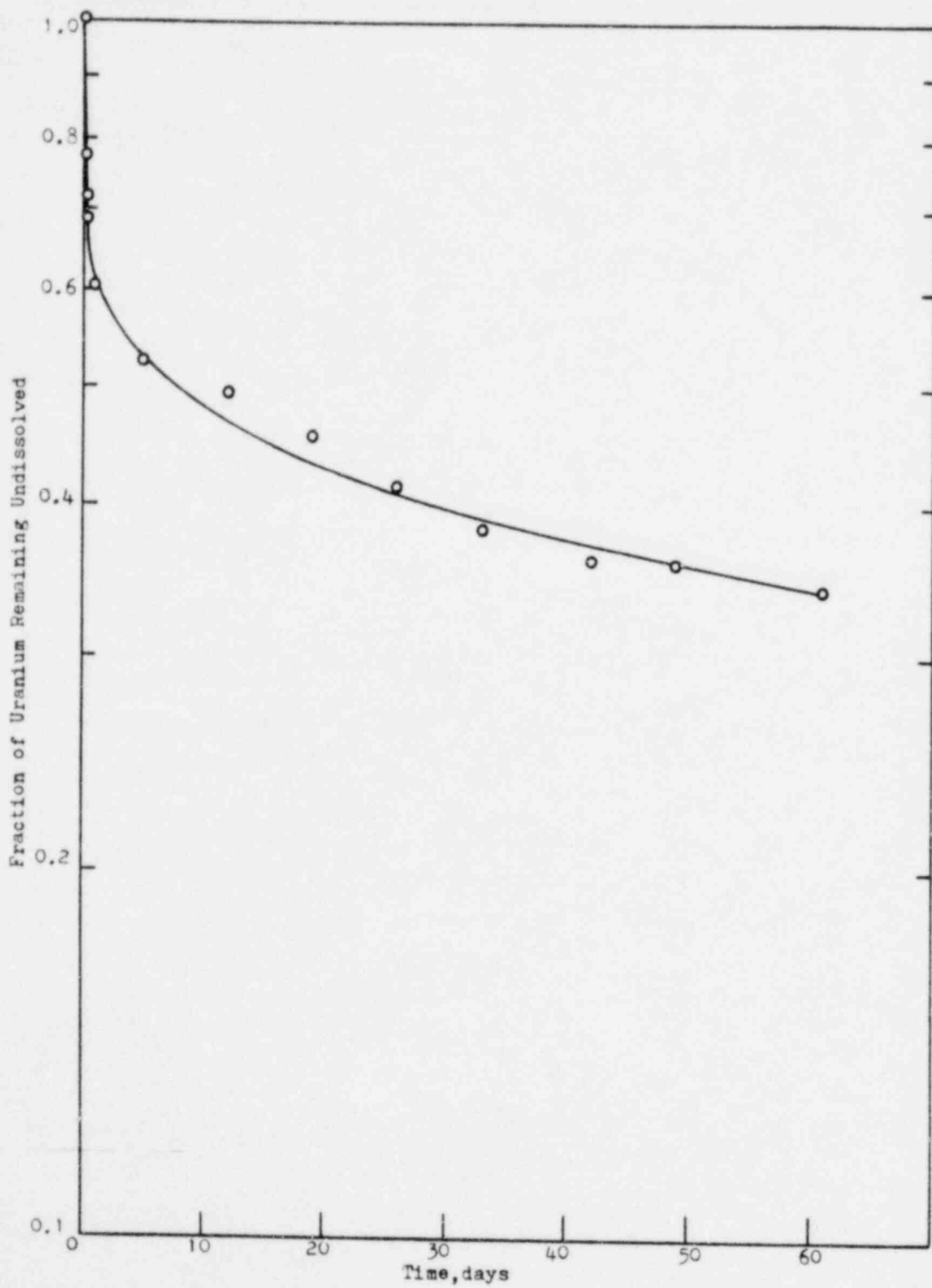


FIGURE 17. Dissolution of Dust, Collected at Babcock & Wilcox's ADU Granulator Discharge, into Simulated Lung Fluid at 37°C

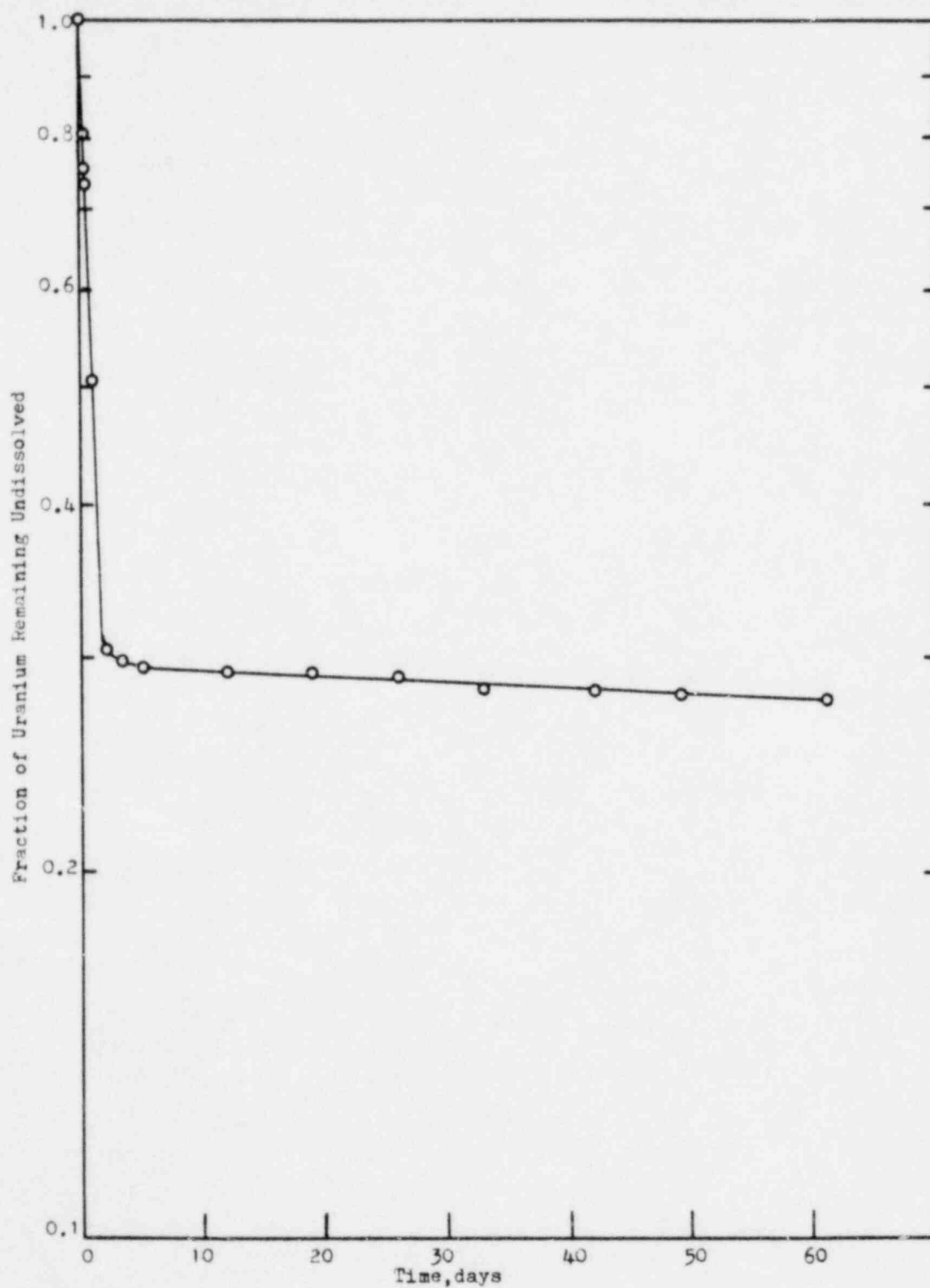


FIGURE 18. Dissolution of Dust, Collected at Babcock & Wilcox's ADU Calciner Discharge, into Simulated Lung Fluid at 37°C

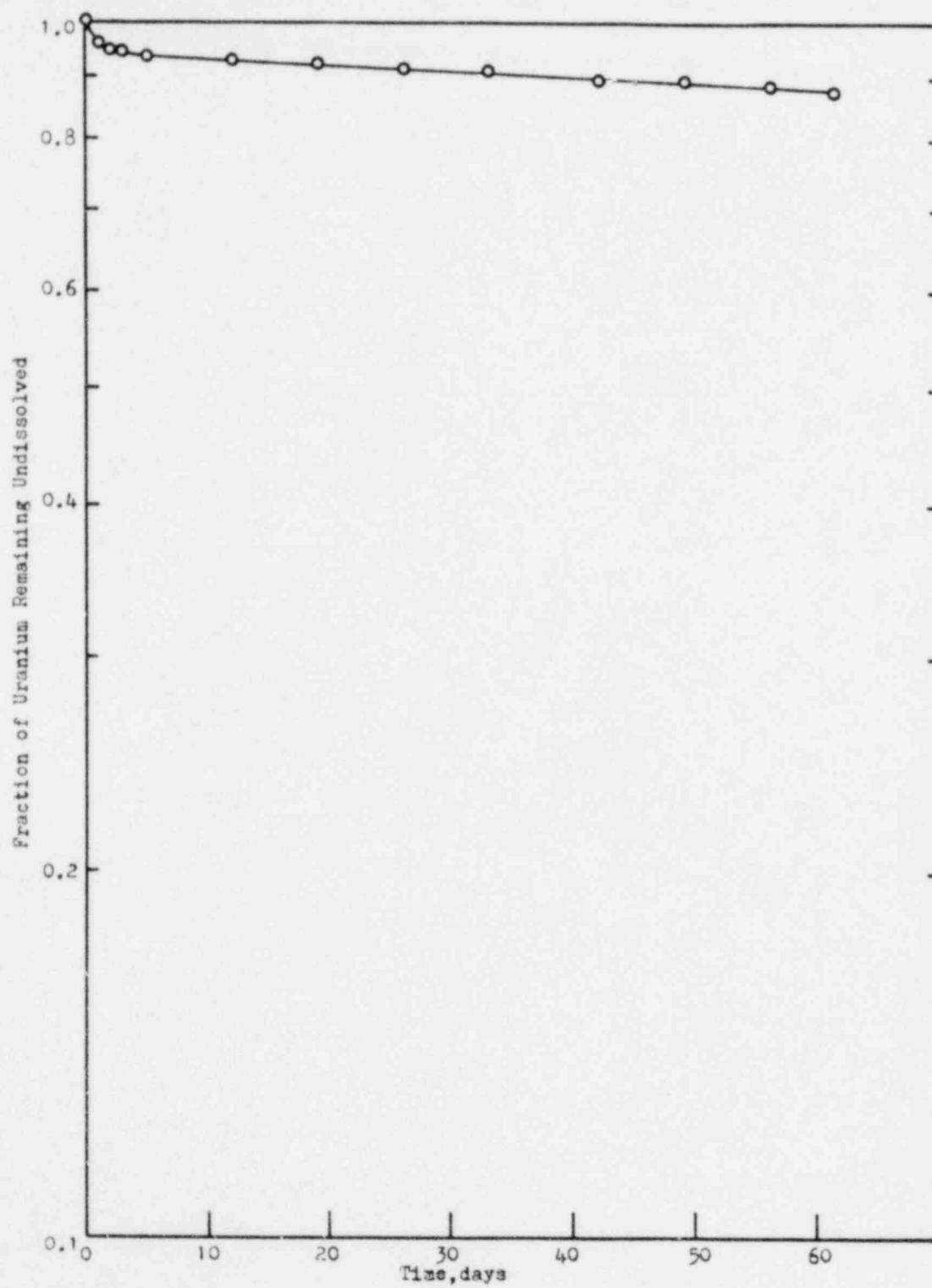


FIGURE 19. Dissolution of Dust, Collected at Babcock & Wilcox's Reduction Kiln Discharge, into Simulated Lung Fluid at 37°C

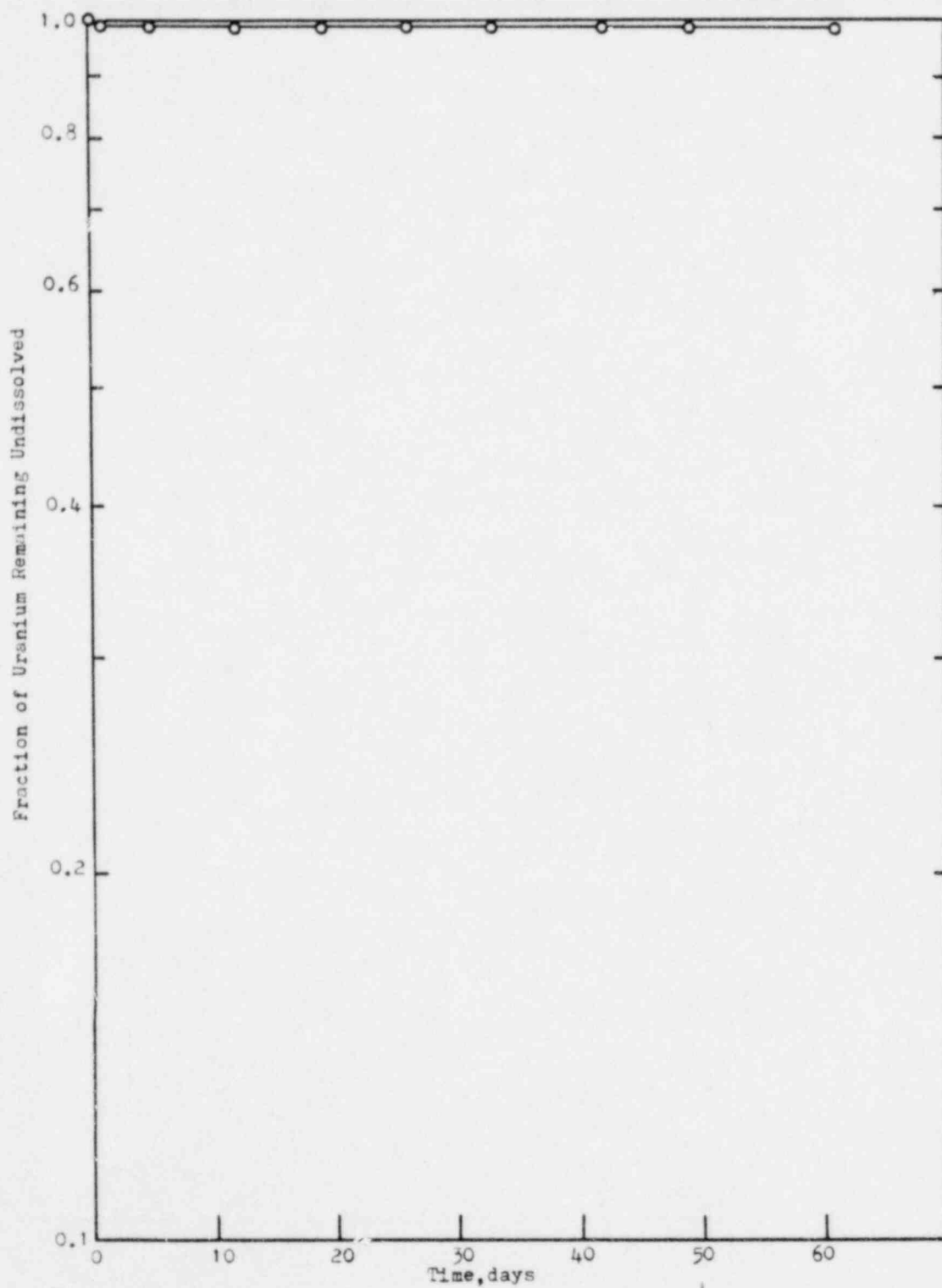


FIGURE 20. Dissolution of Dust, Collected at Babcock & Wilcox's Pellet Grinders, into Simulated Lung Fluid at 37°C

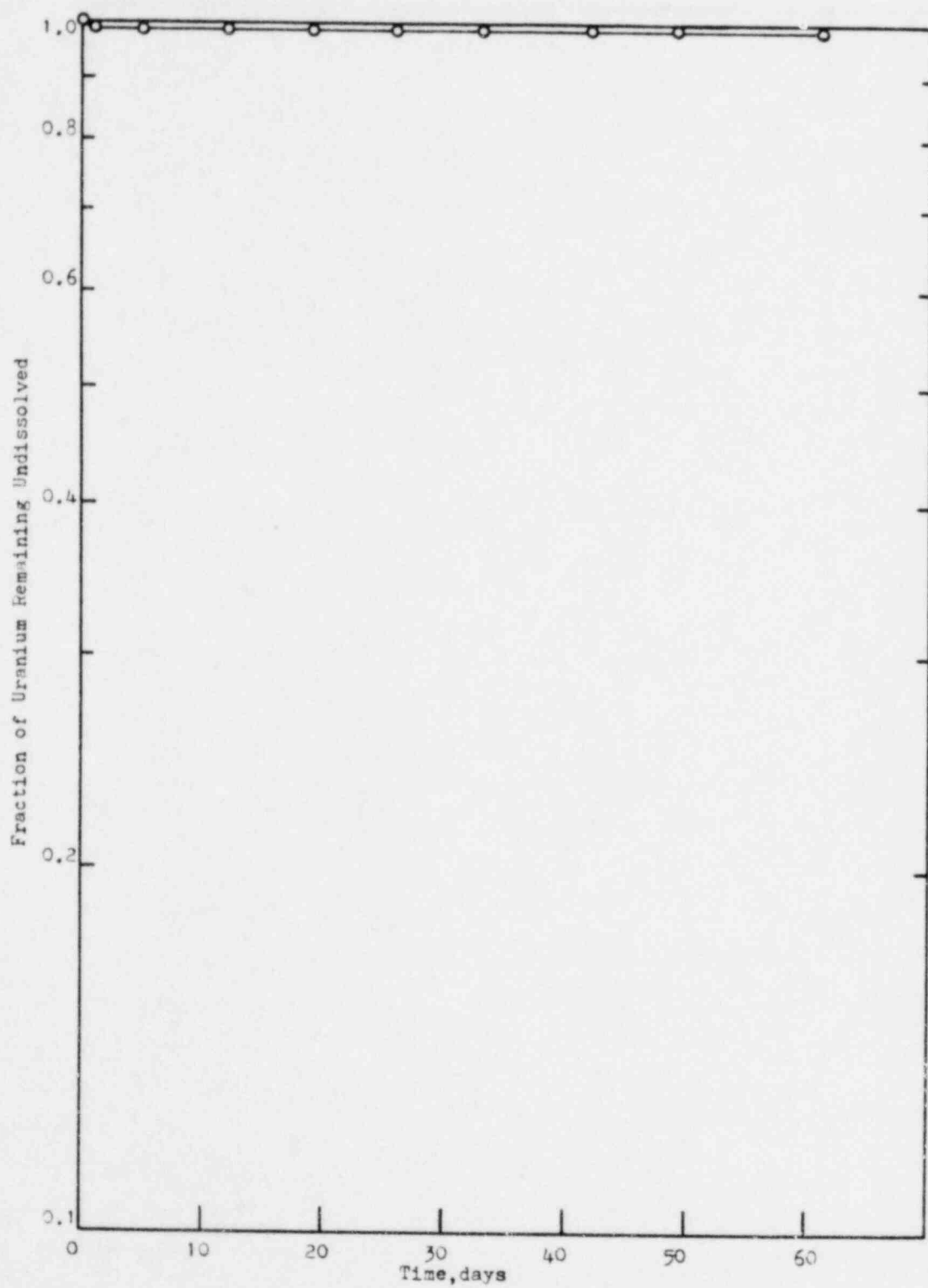


FIGURE 21. Dissolution of Dust, Collected at Babcock & Wilcox's Uranium Scrap Recovery Area, into Simulated Lung Fluid at 37°C

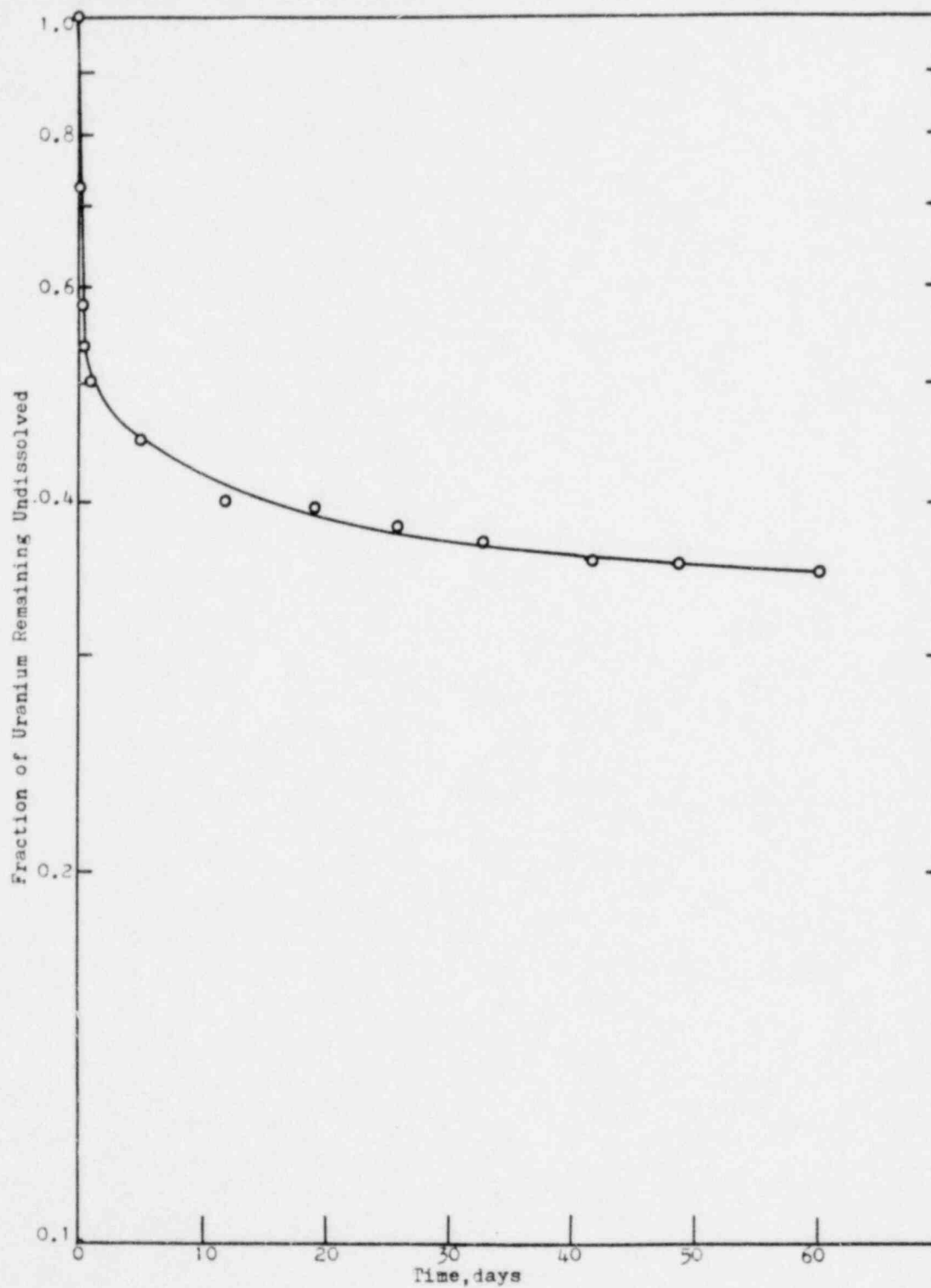


FIGURE 22. Dissolution of Dust, Collected at Babcock & Wilcox's Uranium Scrap Dissolver, into Simulated Lung Fluid at 37°C

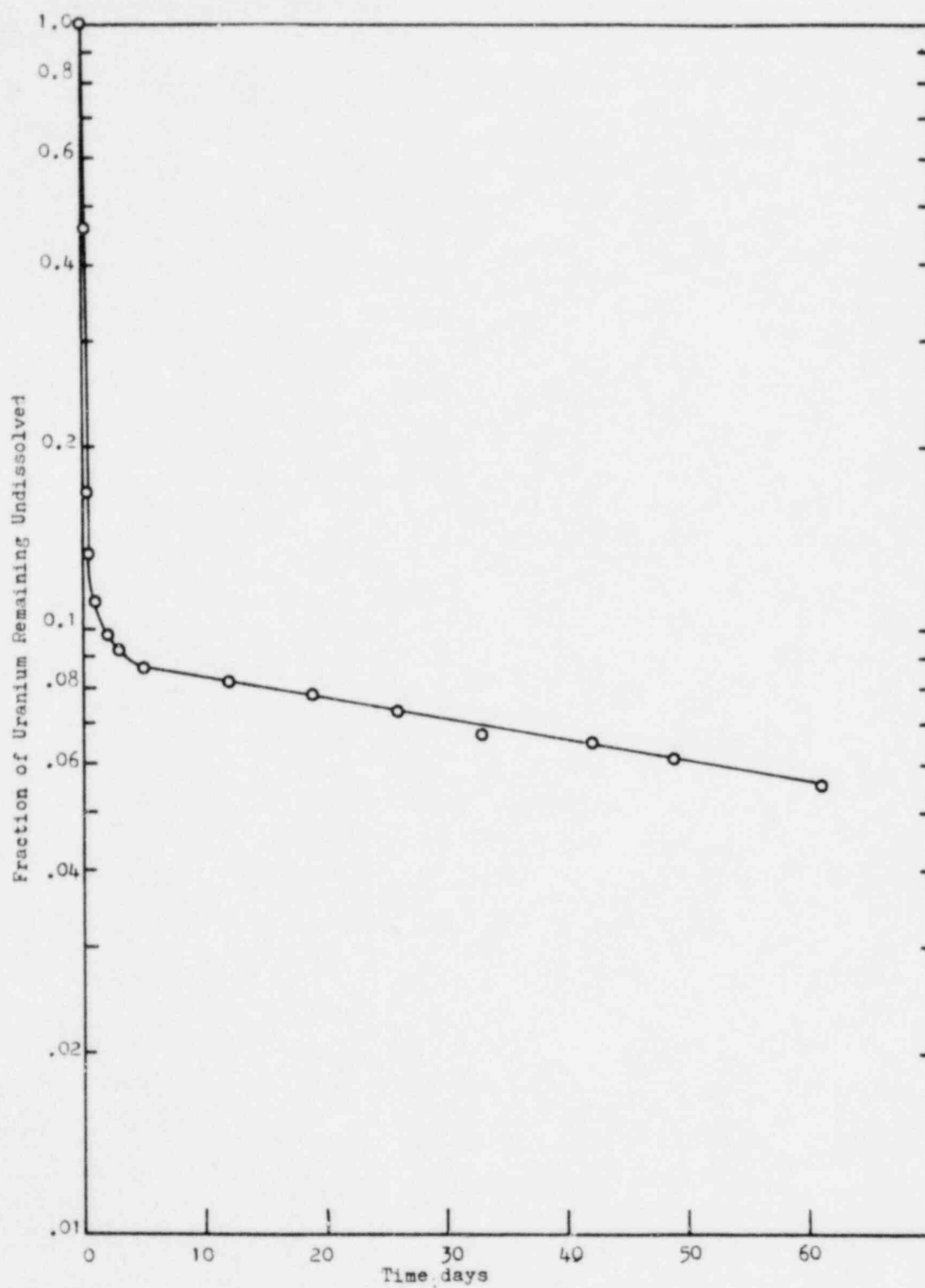


FIGURE 23. Dissolution of Dust, Collected at Westinghouse's ADU Granulator Discharge, into Simulated Lung Fluid at 37°C

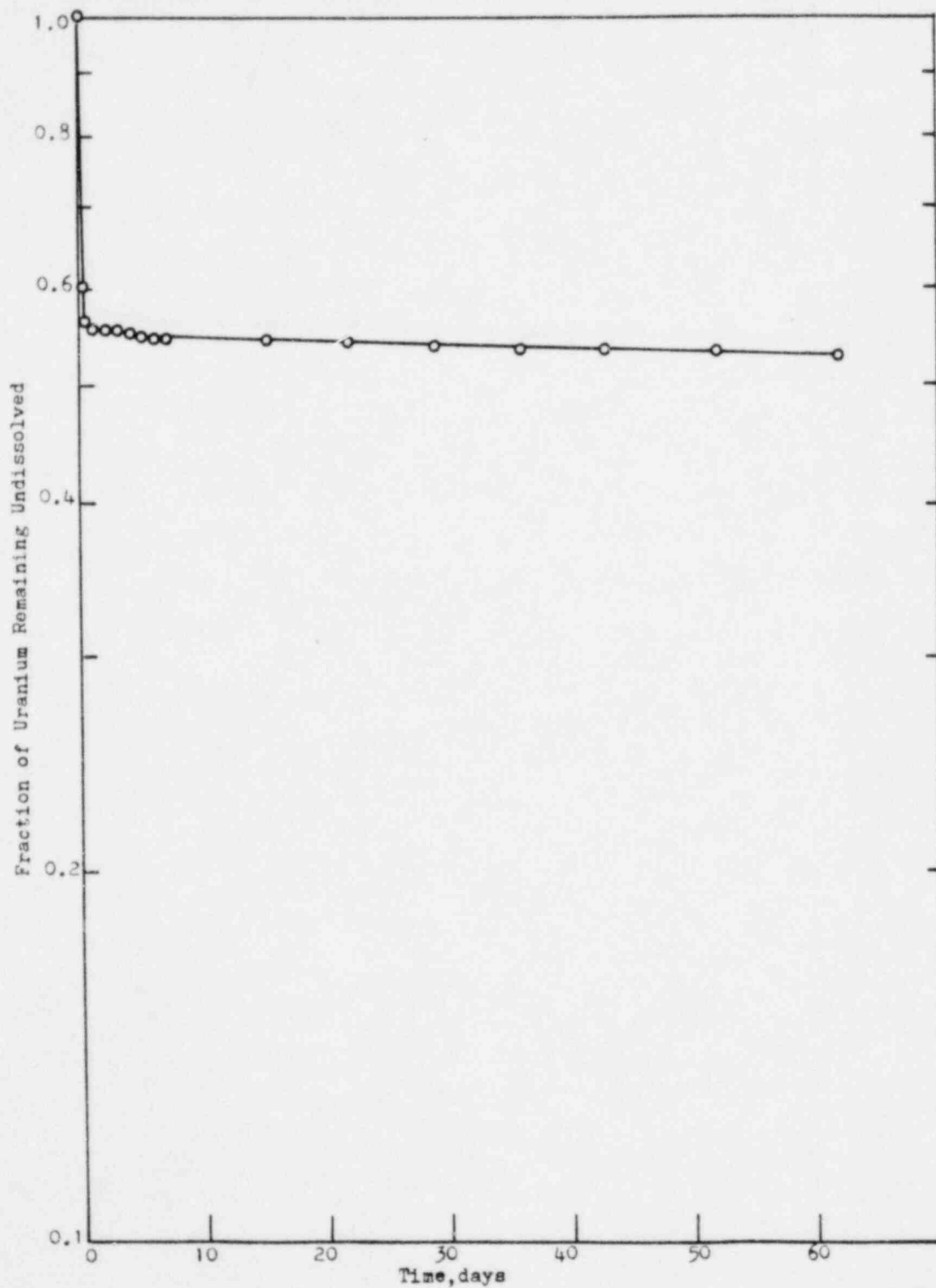


FIGURE 24. Dissolution of Dust Collected at Westinghouse's Sintering Furnace Feed, into Simulated Lung Fluid at 37°C

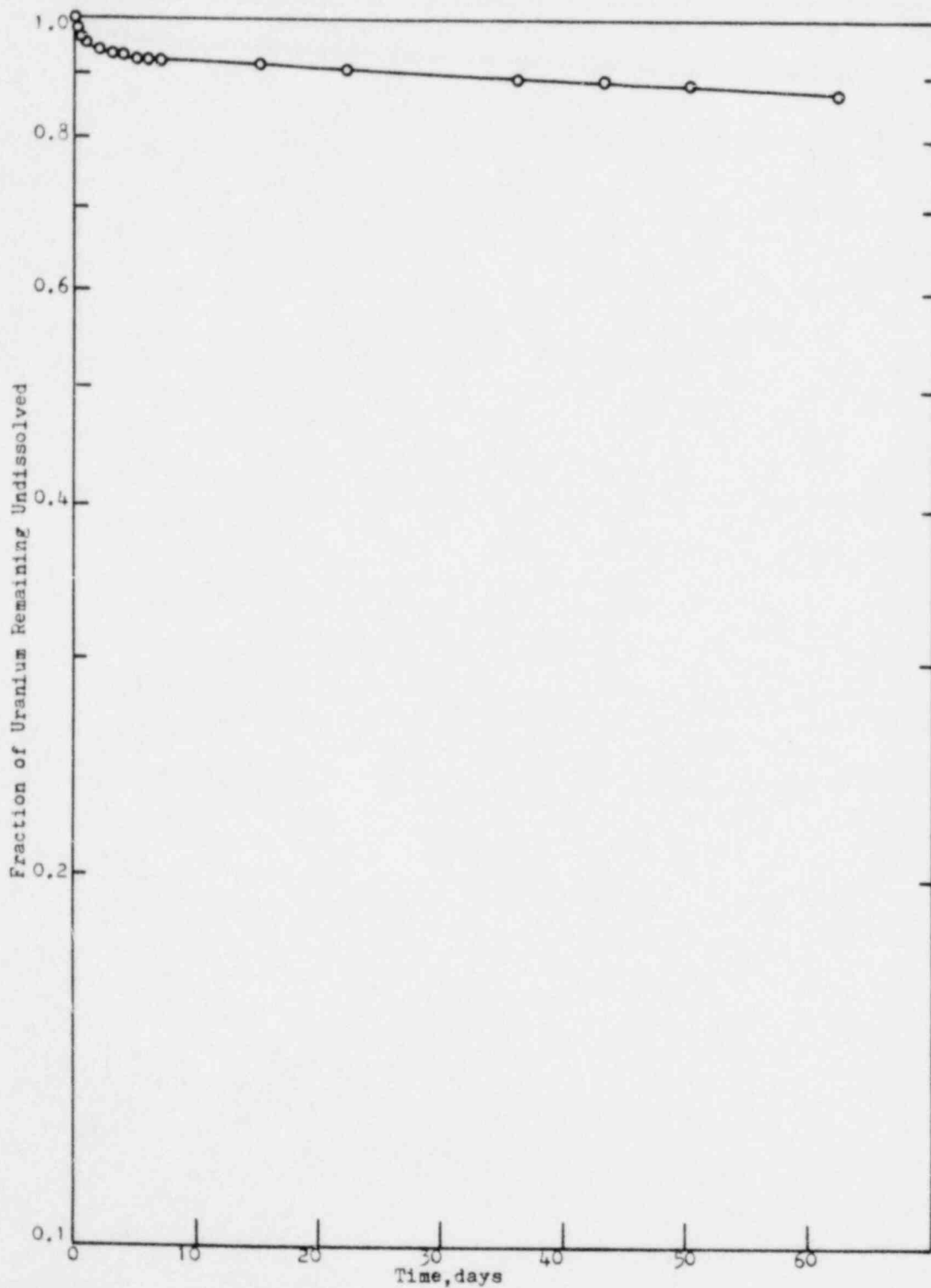


FIGURE 25. Dissolution of Dust Collected at Westinghouse's Uranium Scrap Recovery Area, into Simulated Lung Fluid at 37°C

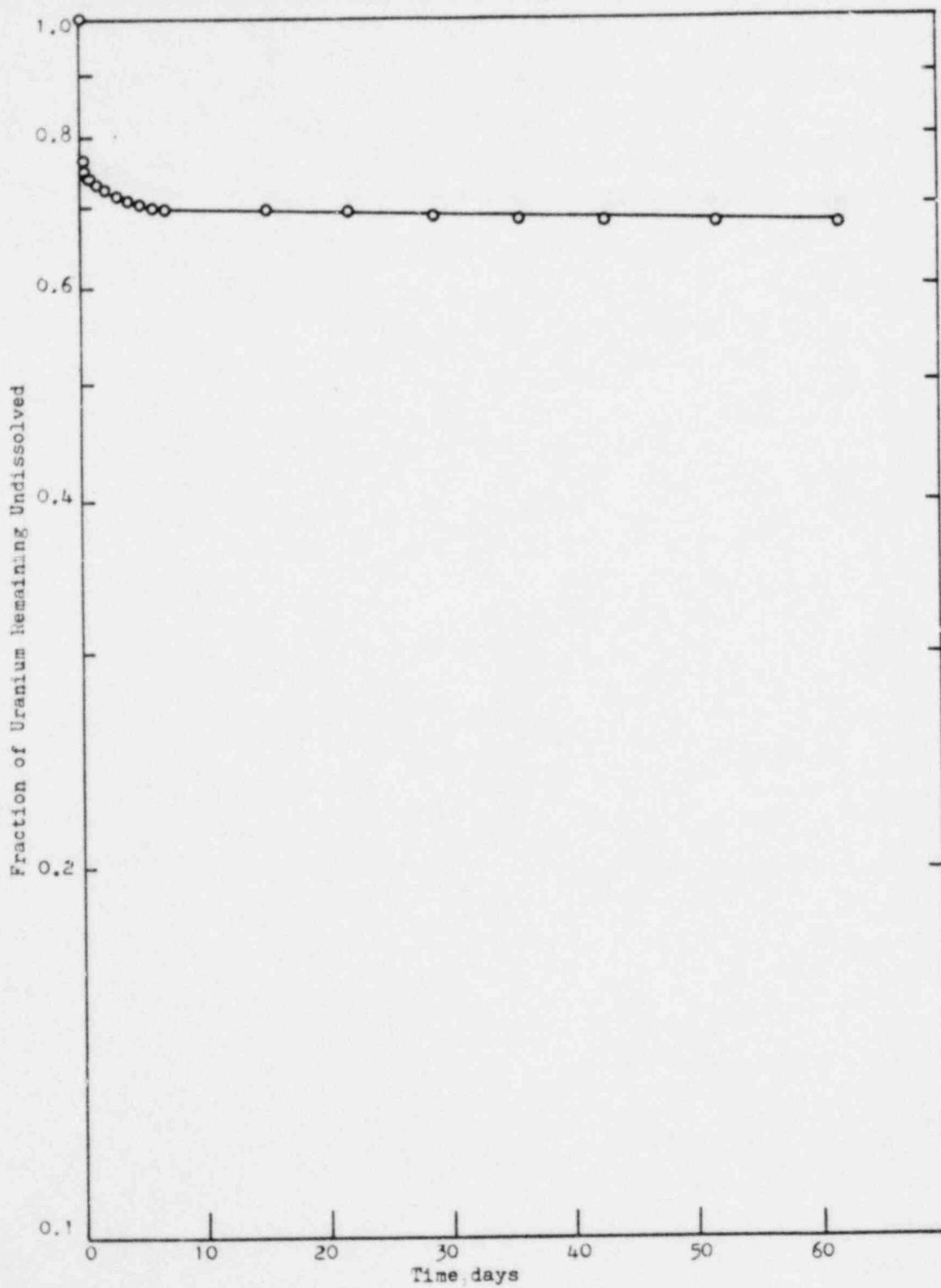


FIGURE 26. Dissolution of Dust Collected at General Electric's UF_6 Vaporization Room, into Simulated Lung Fluid at $37^\circ C$

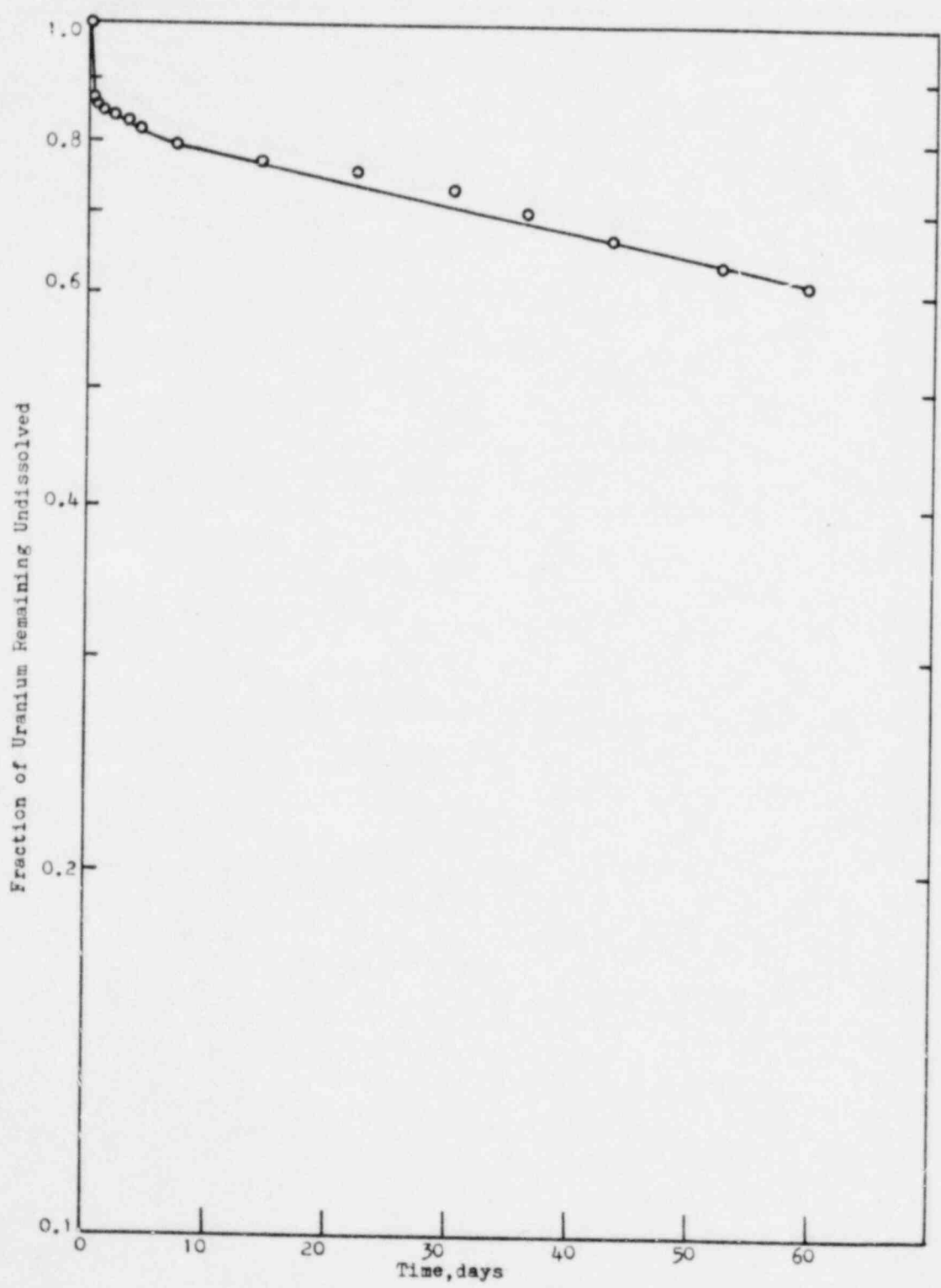


FIGURE 27. Dissolution of Dust, Collected at General Electric's UF_6 Hydrolyzer, into Simulated Lung Fluid at $37^\circ C$

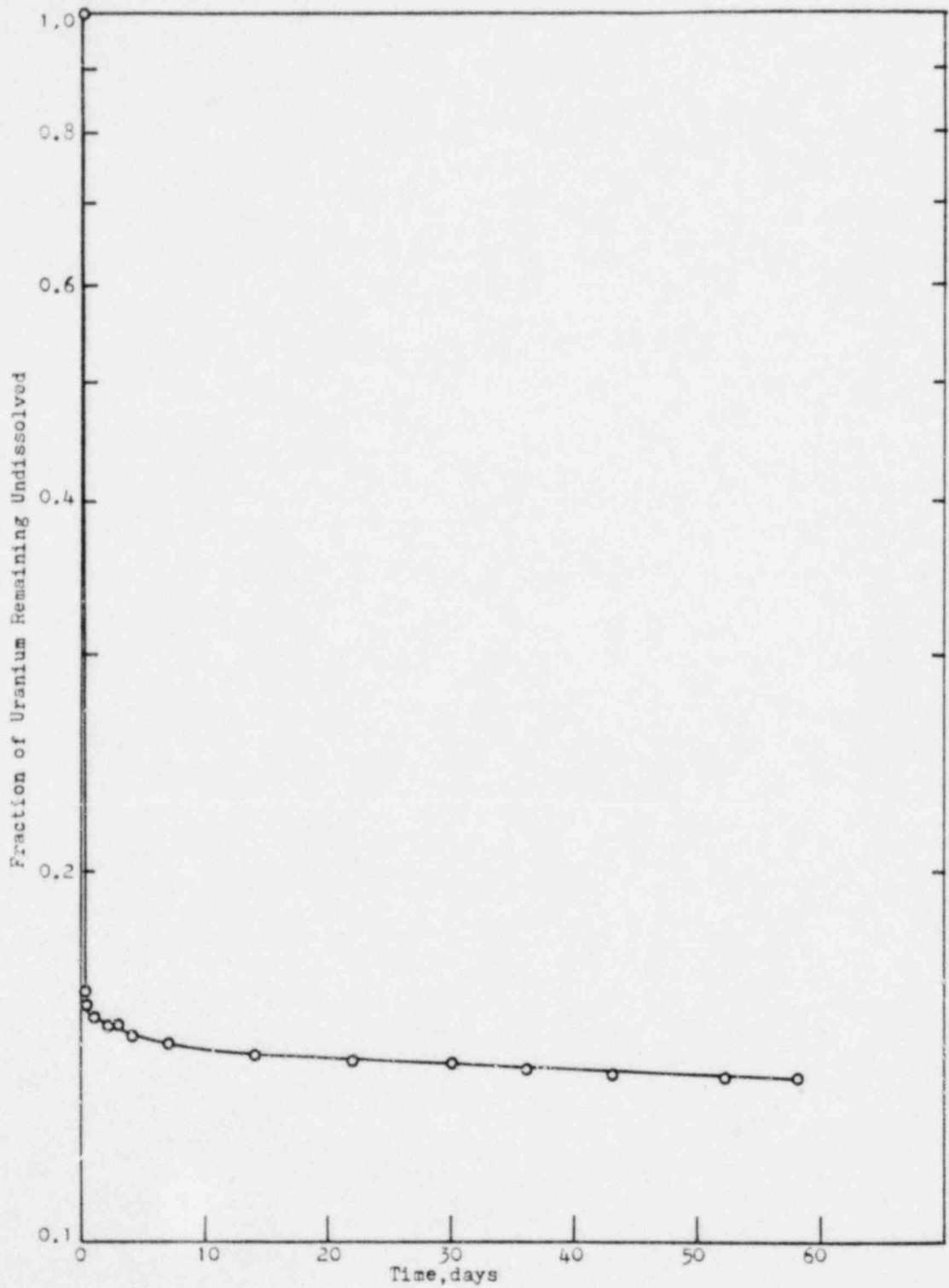


FIGURE 28. Dissolution of Dust, Collected at General Electric's ADU Calciner Feed, into Simulated Lung Fluid at 37°C

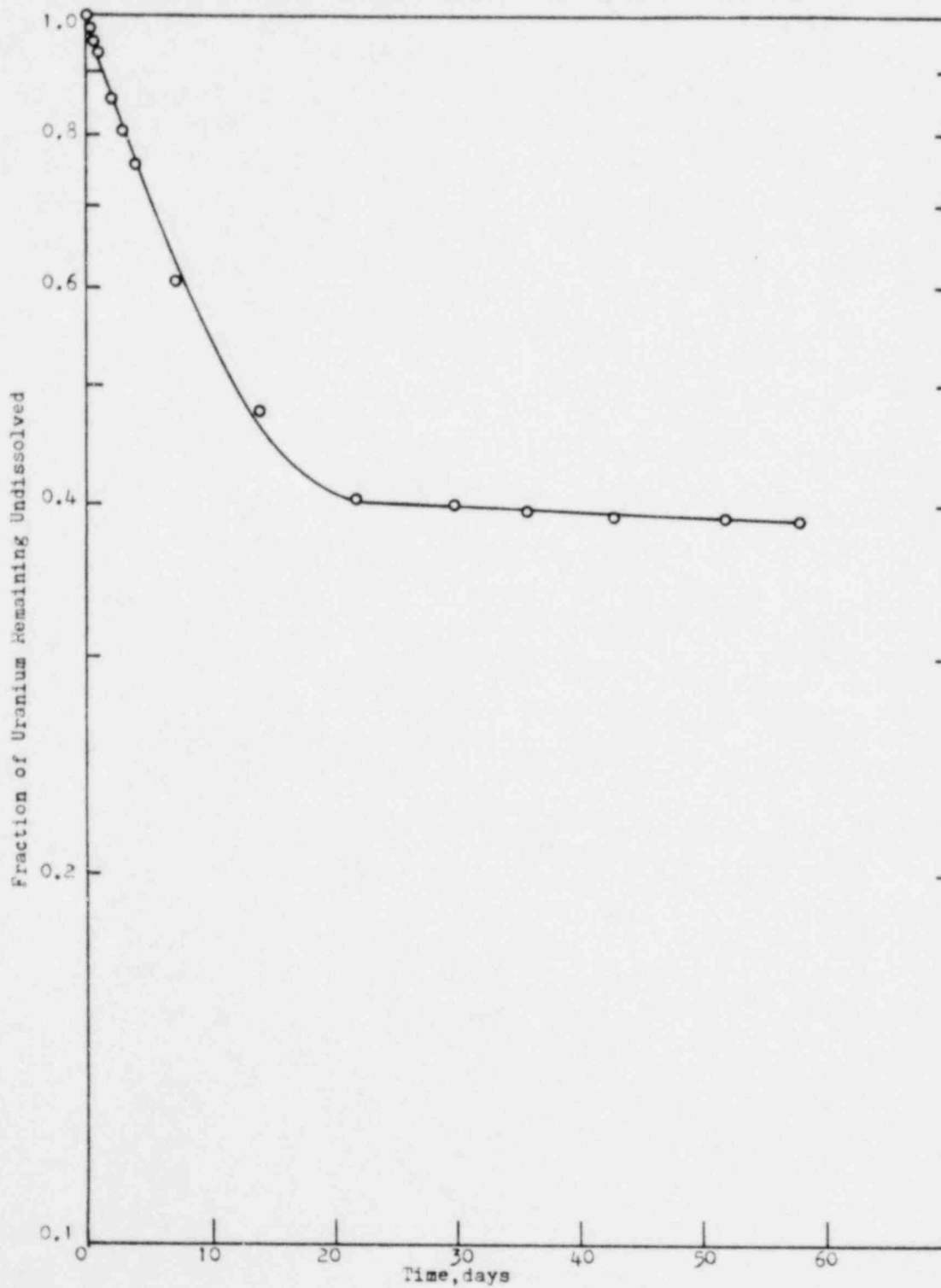


FIGURE 29. Dissolution of Dust, Collected at General Electric's GECO Calciner Feed, into Simulated Lung Fluid at 37°C

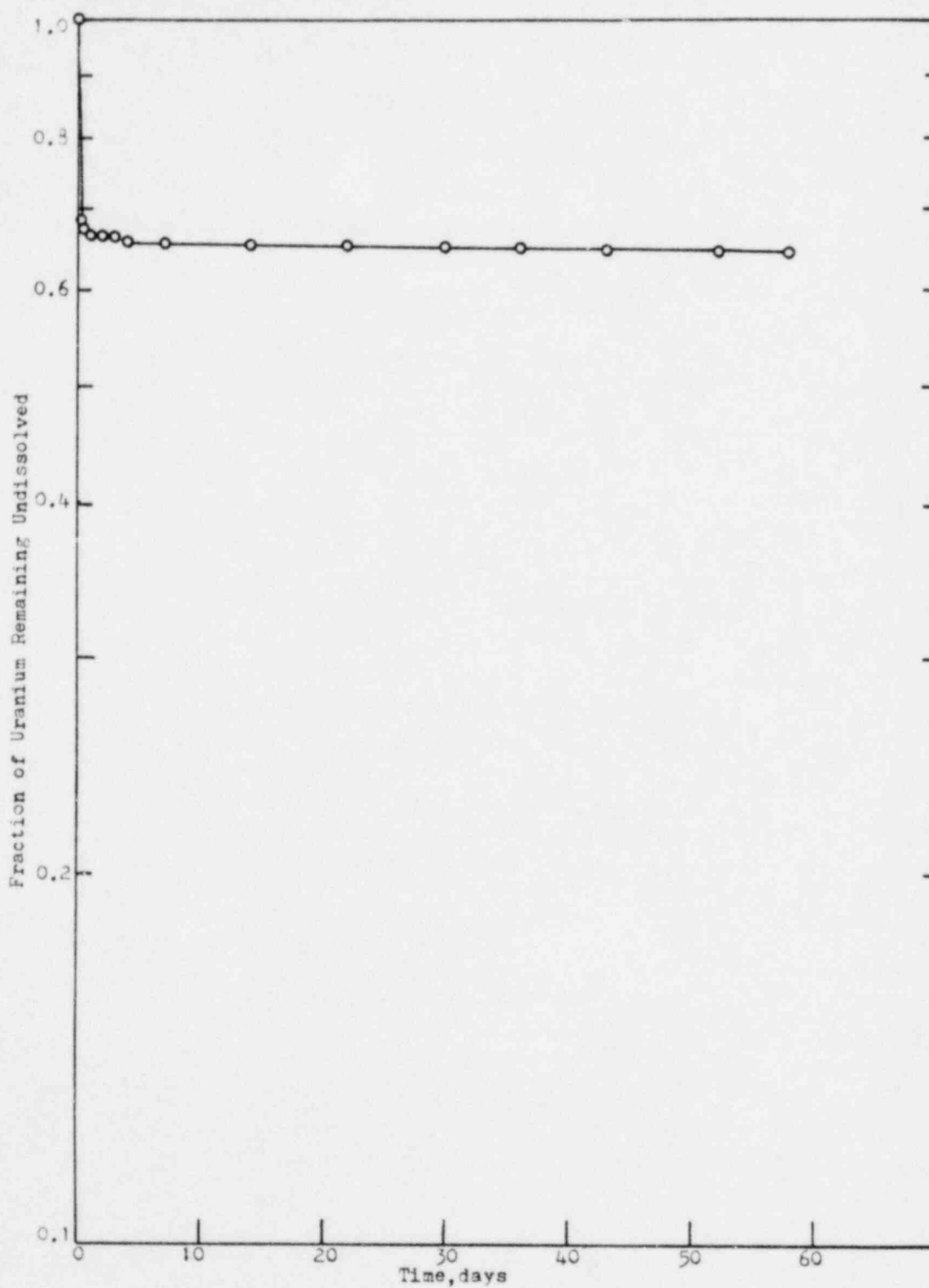


FIGURE 30. Dissolution of Dust Collected at General Electric's ADU Calciner Discharge, into Simulated Lung Fluid at 37°C

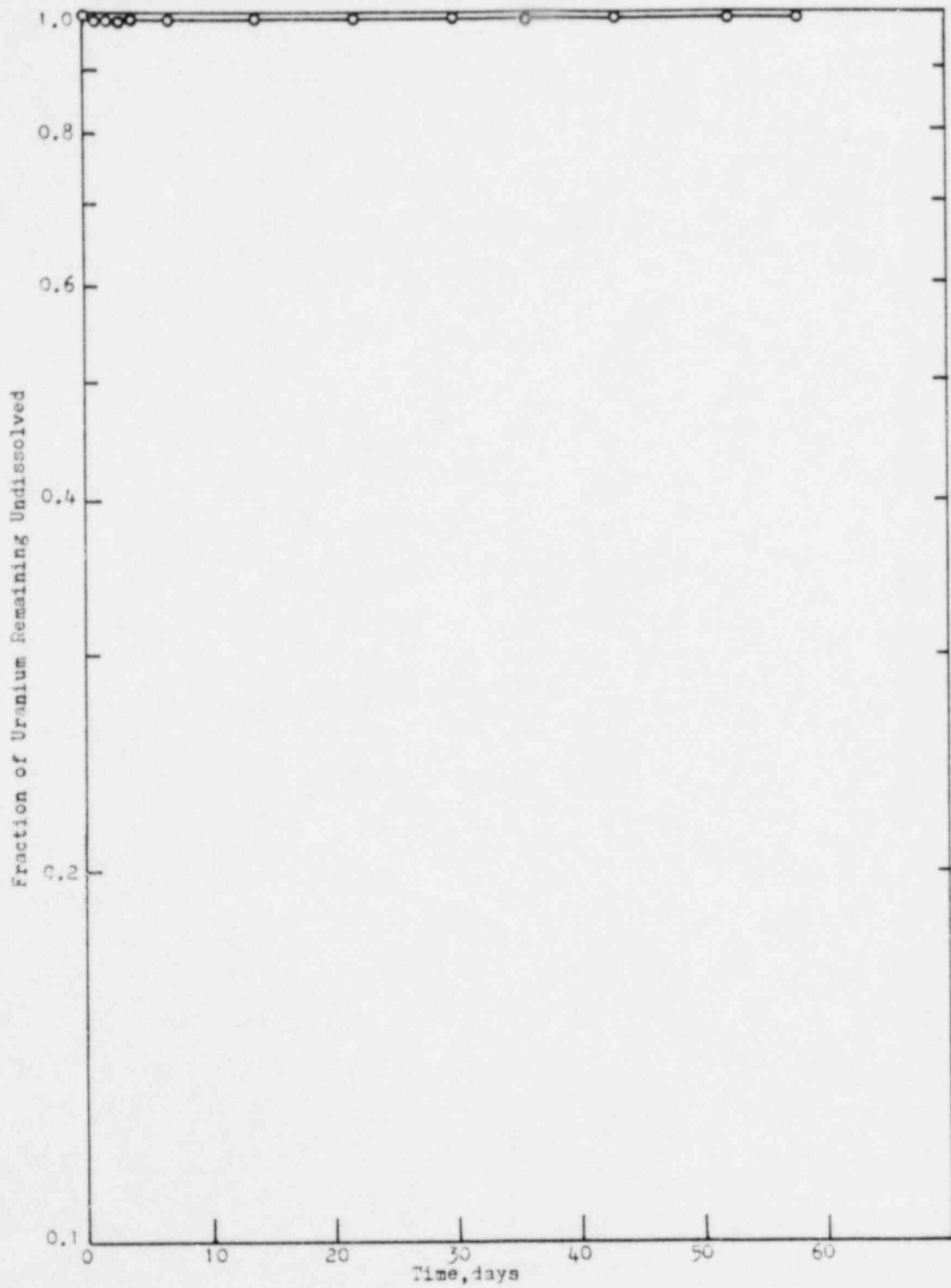


FIGURE 31. Dissolution of Dust Collected at General Electric's GECO Calciner Discharge, into Simulated Lung Fluid at 37°C

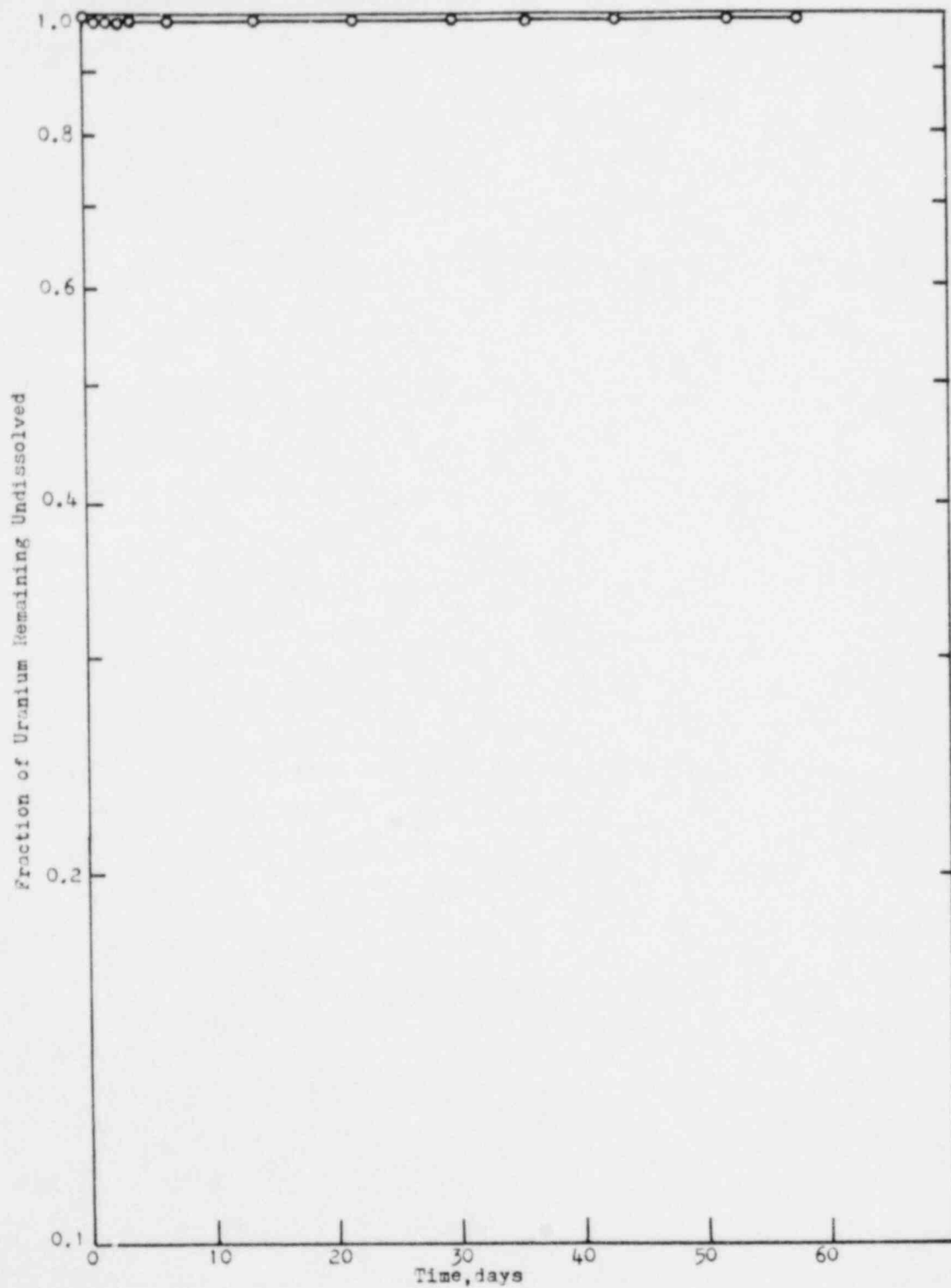


FIGURE 32. Dissolution of Dust Collected at General Electric's Pellet Press, into Simulated Lung Fluid at 37°C

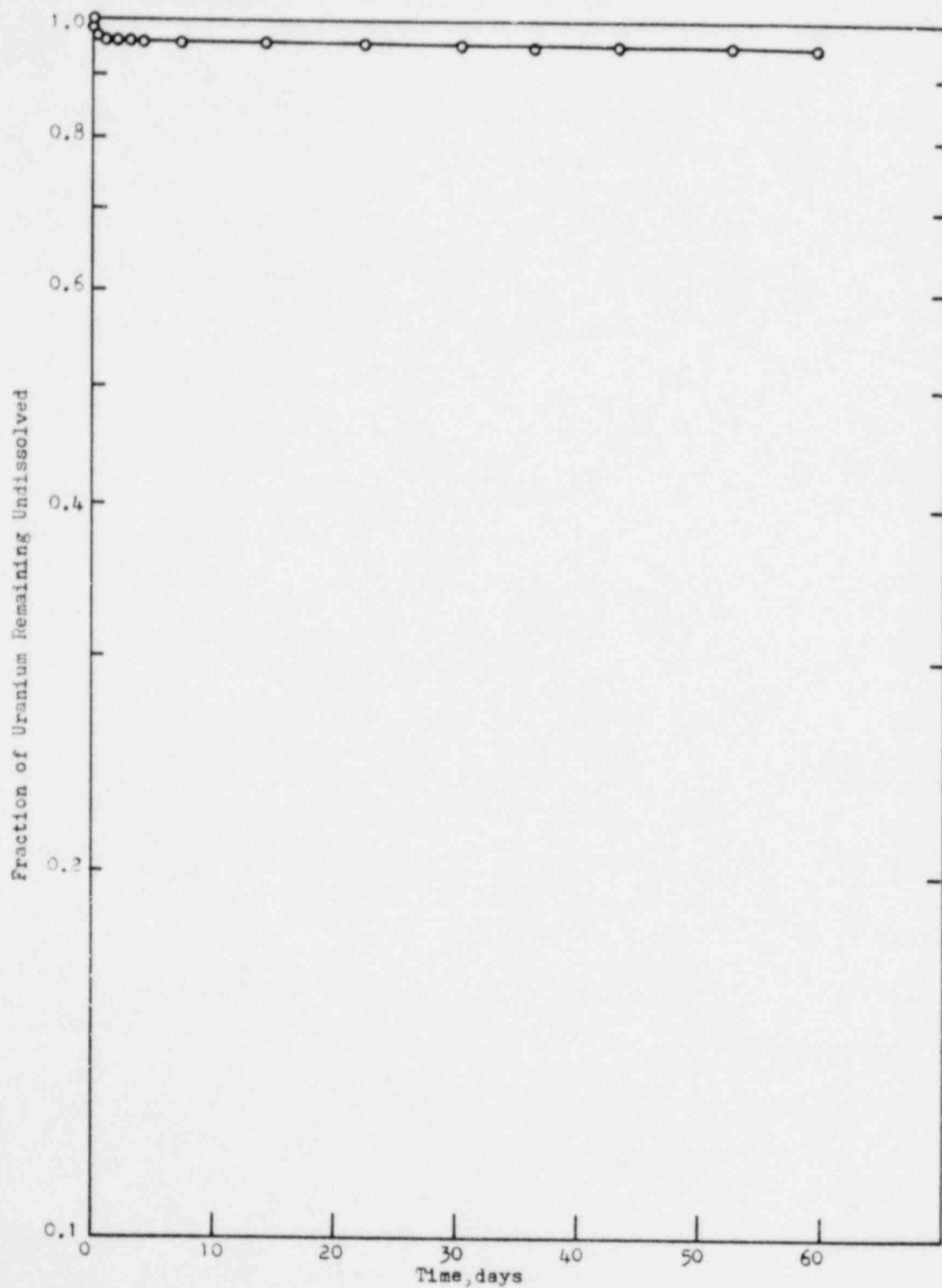


FIGURE 33. Dissolution of Dust Collected at General Electric's Pellet Grinder, into Simulated Lung Fluid at 37°C

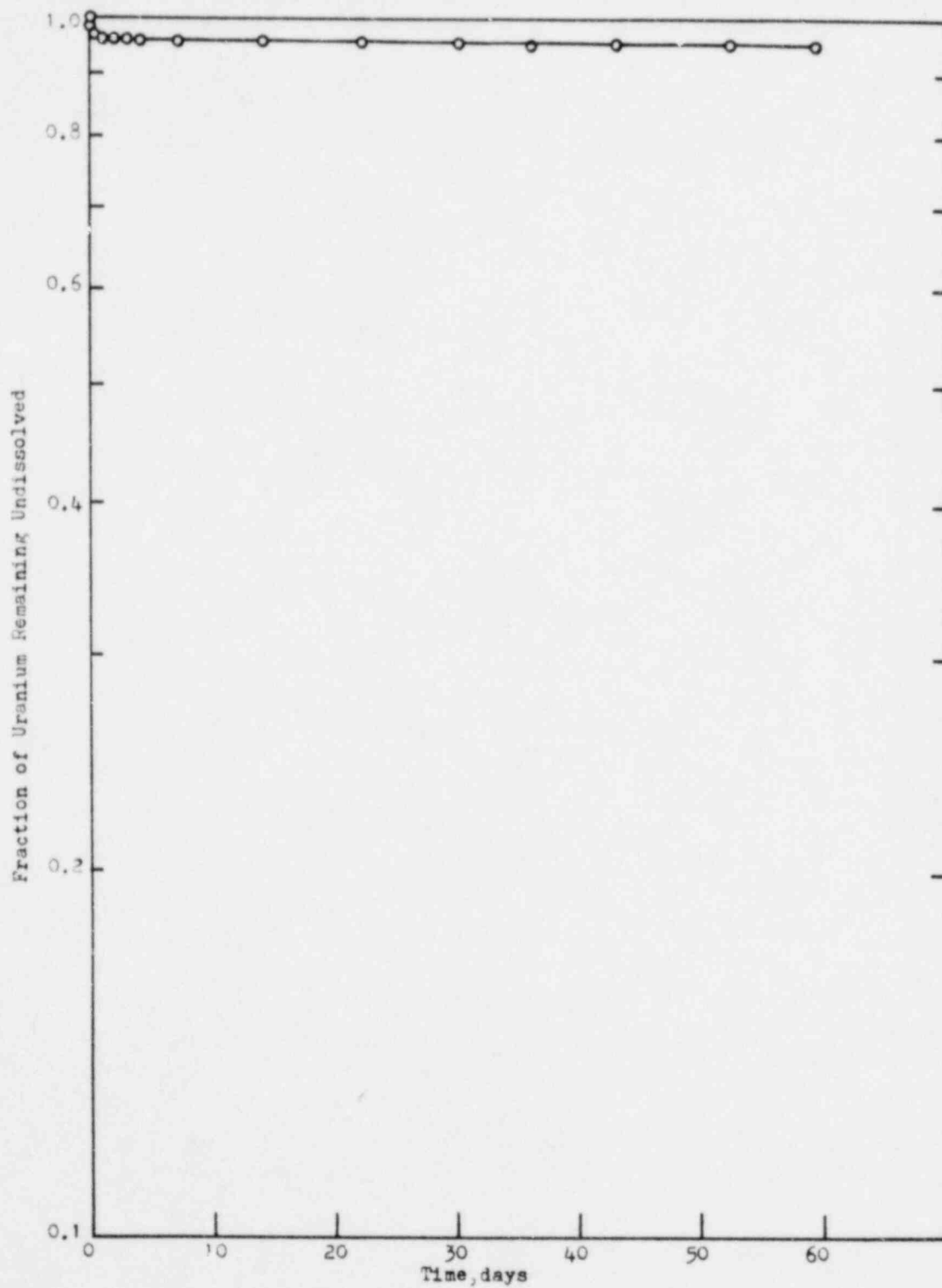


FIGURE 34. Dissolution of Dust Collected at General Electric's Chem Room Air Recirculation Intake, ADU End, into Simulated Lung Fluid at 37°C

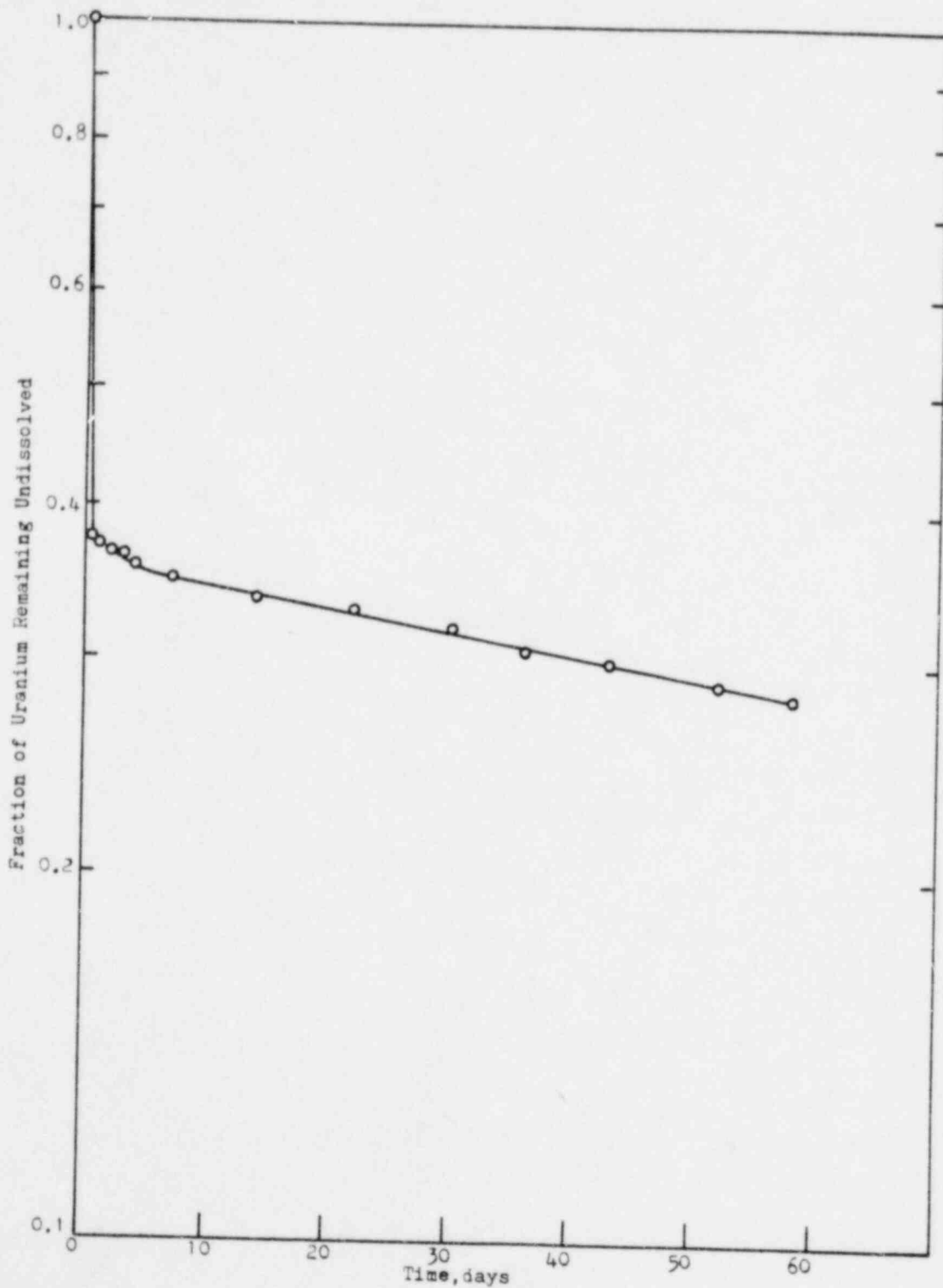


FIGURE 35. Dissolution of Dust Collected at General Electric's Chem Room Air Recirculation Intake, Center, into Simulated Lung Fluid at 37°C

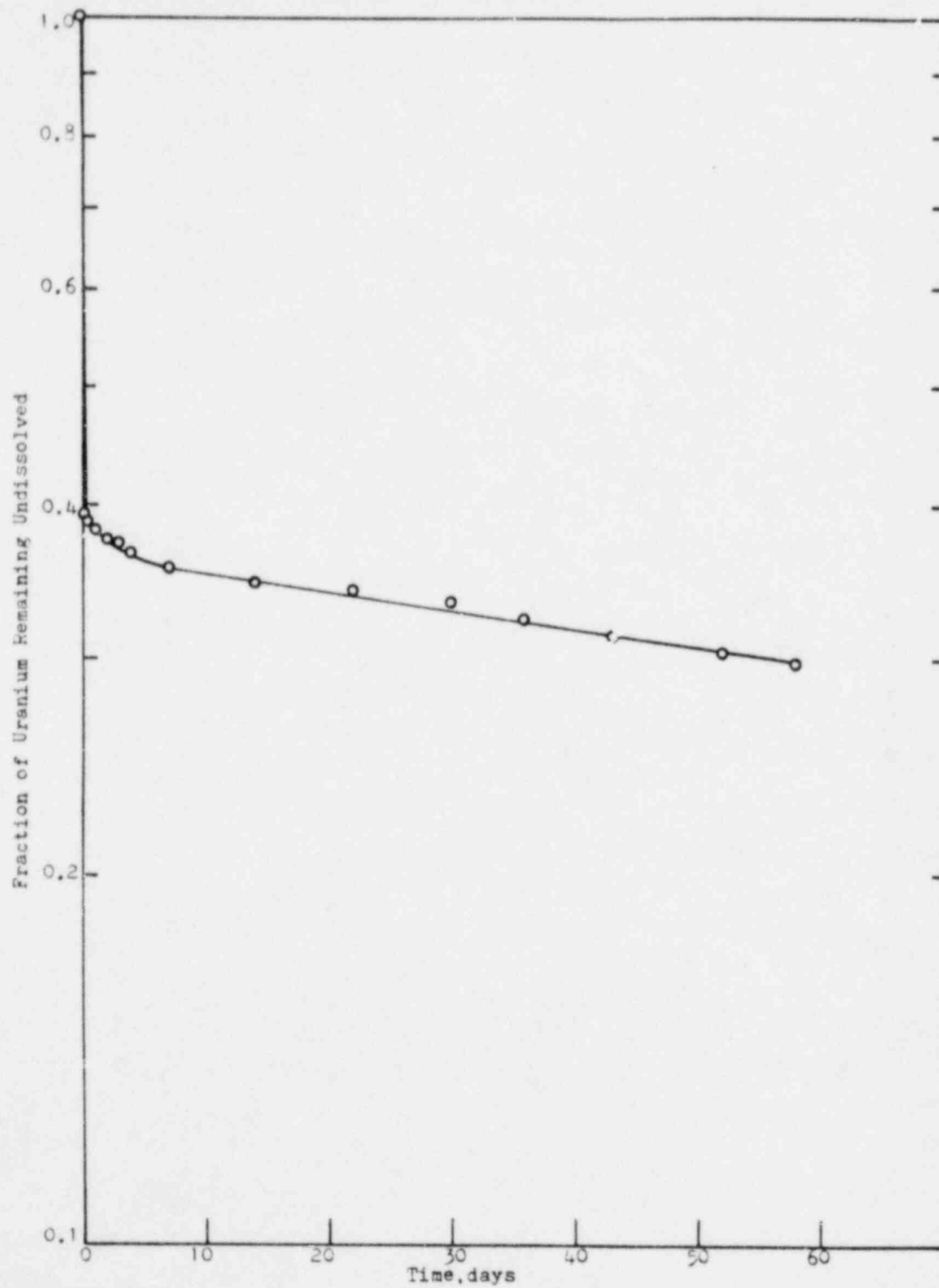


FIGURE 36. Dissolution of Dust Collected at General Electric's Chem Room Air Recirculation Intake, GECCO End, into Simulated Lung Fluid at 37°C

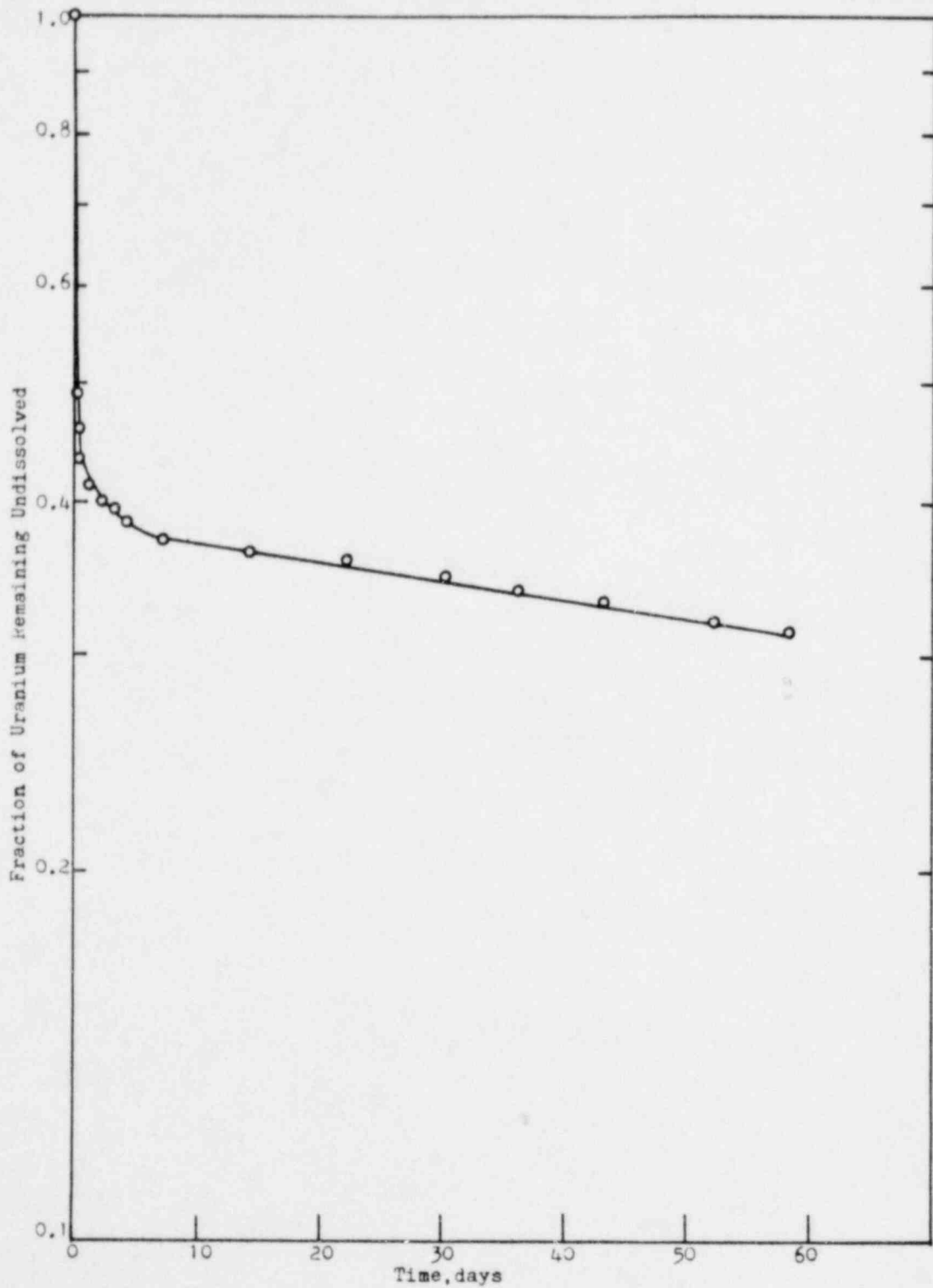
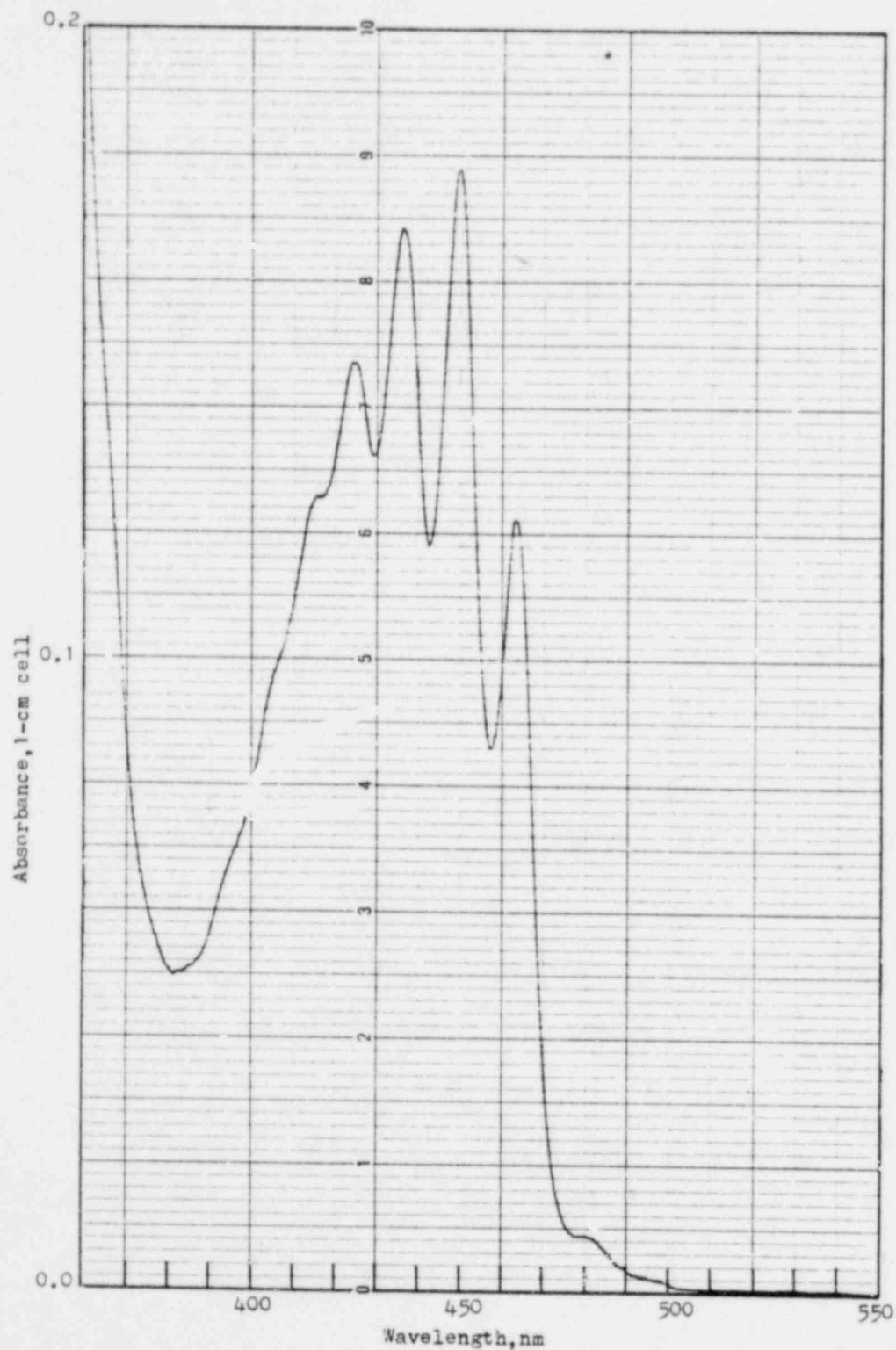


FIGURE 37. Optical Absorption Spectrum of 1.78 g/l Uranium Solution in Simulated Lung Fluid



Sufficient terms were included to fit the data to the precision of the measurements. The results are tabulated in Table 4.

TABLE 4. Weight Fractions and Dissolution Half-times of Uranium Components

Sample	f_1	T_1	f_2	T_2	f_3	T_3
Ammonium diuranate (April 1978)	1.00	0.2d				
Ammonium diuranate (July 1979)	1.00	2.0d				
Ammonium diuranate (March 1980)	1.00	5.0d				
Uranium trioxide (batch)	0.45	0.5d	0.55	123d		
Uranium trioxide (mini- batch)	0.51	0.7d	0.49	184d		
Uranium octoxide	1.00	∞				
Uranium dioxide	1.00	∞				
Uranium tetrafluoride	1.00	∞				
<u>Exxon Plant Dust</u>						
ADU granulator discharge	0.70	0.4d	0.30	1,256d		
ADU reduction-kiln dis- charge	1.00	∞				
Pellet grinder	1.00	∞				
U scrap recovery area	1.00	∞				
<u>Babcock and Wilcox Plant Dust</u>						
UF ₆ hydrolyzer	0.28	0.4d	0.18	0.8d	0.54	82d
ADU granulator discharge	0.13	0.01d	0.59	0.6d	0.28	∞
ADU calciner discharge	0.02	0.07d	0.04	1.0d	0.94	600d
U ₃ O ₈ reduction kiln discharge	0.01	0.01	0.99	11,300d		
Pellet grinder	0.01	0.01	0.99	10,316d		
U scrap recovery area	0.50	0.01	0.11	5.4d	0.39	323d
U scrap dissolver	0.91	0.08d	0.09	80d		
<u>Westinghouse Plant Dust</u>						
ADU calciner discharge	0.44	0.02d	0.01	1.6d	0.55	1039d
Sintering furnace dis- charge	0.03	0.03d	0.04	1.4d	0.93	664d
U scrap recovery area	0.25	0.03d	0.05	1.7d	0.70	1063d
<u>General Electric Plant Dust</u>						
UF ₆ vaporization room	0.13	0.03d	0.04	1.3d	0.83	137d
UF ₆ vaporizer/dissolver	0.89	0.01d	0.02	2.4d	0.09	172d

TABLE 4 (continued)

Sample	f_1	T_1	f_2	T_2	f_3	T_3
<u>General Electric Plant Dust (continued)</u>						
ADU calciner feed	0.63	5.3d	0.37	∞		
GECO calciner feed	0.32	0.02d	0.02	1.4d	0.66	2391d
ADU calciner discharge	0.01	0.01d	0.99	∞		
GECO calciner discharge	0.01	0.01d	0.99	∞		
Pellet press	0.04	0.01d	0.96	∞		
Pellet grinder	0.03	0.01d	0.97	∞		
Chem room air, ADU end	0.54	0.04d	0.07	0.92d	0.39	189d
Chem room air, center	0.61	0.02d	0.03	1.8d	0.37	196d
Chem room air, GECO end	0.52	0.02d	0.02	1.9d	0.36	167d

SOLUBILITY CLASSIFICATIONS OF SAMPLES

On the basis of the dissolution half-times of the samples listed in Table 4, their dissolution rates were classified in terms of the ICRP Task Group Lung Model as shown in Table 5.

TABLE 5. Dissolution-rate Classifications of Samples in Terms of the ICRP Task Group Lung Model

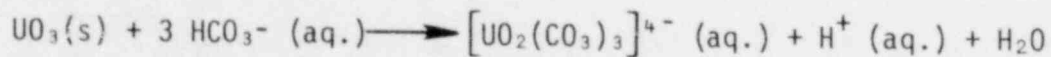
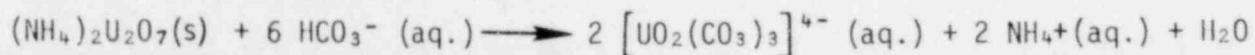
Sample	Classification
Ammonium diuranate	D
Uranium trioxide	48% D, 52% Y
Uranium octoxide	Y
Uranium dioxide	Y
Uranium tetrafluoride	Y
<u>Exxon Plant Dust</u>	
ADU granulator discharge	70% D, 30% Y
ADU reduction kiln discharge	Y
Pellet grinder	Y
U scrap recovery	Y
<u>Babcock and Wilcox Plant Dust</u>	
UF ₆ hydrolyzer	46% D, 54% W
ADU granulator discharge	72% D, 28% Y
ADU calciner discharge	6% D, 94% Y
U ₃ O ₈ reduction kiln discharge	1% D, 99% Y
Pellet grinder	1% D, 99% Y
U scrap recovery area	6% D, 39% Y
U scrap dissolver	91% D, 9% W

TABLE 5 (continued)

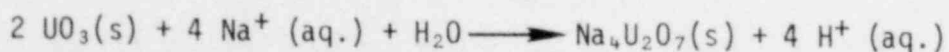
<u>Sample</u>	<u>Classification</u>
ADU calciner feed	45% D, 55% Y
Sintering furnace discharge	7% D, 93% Y
U scrap recovery area	30% D, 70% Y
<u>General Electric Plant Dust</u>	
UF ₆ vaporizer	17% D, 83% Y
UF ₆ vaporizer/dissolver	91% D, 9% Y
ADU calciner feed	63% D, 37% Y
GECO calciner feed	34% D, 66% Y
ADU calciner discharge	1% D, 99% Y
GECO calciner discharge	1% D, 99% Y
Pellet press	4% D, 96% Y
Pellet grinder	3% D, 97% Y
Chem room air, ADU end	61% D, 39% Y
Chem room air, center	64% D, 36% Y
Chem room air, GECO end	64% D, 36% Y

DISCUSSION

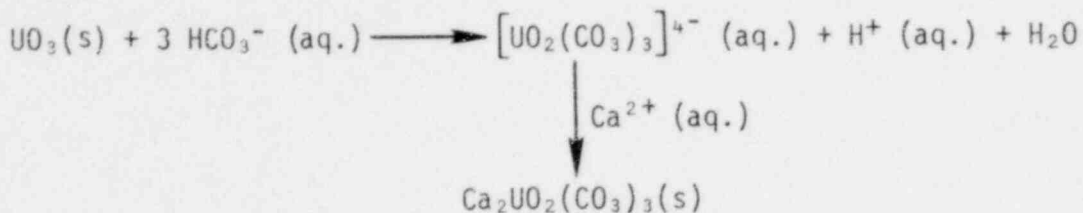
Understanding of the dissolution behavior of even pure uranium compounds requires considerable information on their reactions with the components of either simulated or actual lung fluid. Only a portion of this information could be developed within the scope of the present work. The optical absorption spectrum of the solutions surrounding the dust samples provided an important clue concerning the dissolution mechanism. As stated previously, this spectrum, shown in Figure 37, coincides with that for the $[\text{UO}_2(\text{CO}_3)_3]^{4-}$ anion. Thus, reasonable mechanisms for the dissolution of ammonium diuranate and uranium trioxide in SLF are:



The non-exponential decrease in the fraction of UO_3 found remaining undissolved in SLF may be due to one or more reasons. It has been pointed out that UO_3 is not a stable solid phase in the presence of large concentrations of cations.¹⁵ This instability has been attributed to the greater insolubility of uranates as compared with UO_3 , e.g.,

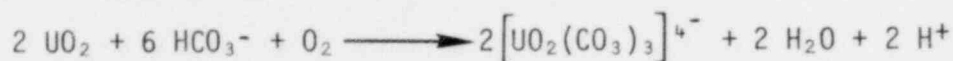


Alternatively, the surface of UO_3 crystals may be such that the calcium ion in SLF may react there to form insoluble calcium uranyl carbonate¹⁶, e.g.,



The kinetics of the competing dissolution and reprecipitation processes may be such that considerable UO_3 may dissolve before the remaining crystals are completely coated with $\text{Ca}_2\text{UO}_2(\text{CO}_3)_3$.

Dissolution of tetravalent uranium compounds requires the presence of oxygen as an oxidizing agent¹⁷, e.g.,



Although the tetravalent compounds were exposed to air-saturated solutions of SLF throughout the dissolution process, it seems possible that the oxidation of uranium surfaces at such an oxygen tension may be quite slow and account for the long dissolution half-times of these compounds. Such conditions, of course, would also prevail in the lung.

COMPARISON OF CLASSIFICATIONS WITH LITERATURE VALUES

There is general agreement that uranium hexafluoride, UF_6 , uranyl nitrate, $\text{UO}_2(\text{NO}_3)_2$, and uranyl fluoride, UO_2F_2 , are Class D compounds¹⁸⁻²⁰. Thus, pure samples of these compounds, which are expected to be airborne in LWR-fuel plants, were not investigated in this study.

Ammonium diuranate has been assigned by others to Class W^{19,20}, but the evidence for this work is that the classification may well depend on the age of the product and its thermal history. The sample used in this study continued to demonstrate Class D behavior over a two-year period, but it was obviously approaching the status of a Class W compound. Ammonium diuranate is known to undergo rapid decomposition at 300°C to form uranium trioxide and ammonia.²¹ It seems possible that a similar slow reaction could occur at the surface of ammonium diuranate at room temperature to convert it from a Class D compound to a Class W one. A more rapid transformation of this could occur in ADU driers and granulators.

Pure uranium trioxide was assigned to a mixed class 48% D, 52% Y in this work. In other reports, this compound has been assigned to the W class^{19,20,22,23}. Possible reasons for the mixed classification of this compound have been discussed under DISSOLUTION MECHANISM.

Both uranium dioxide and uranium octoxide were assigned Class Y from this work, and similar classifications were made on the basis of two other studies reported in the literature^{19,24}. U_3O_8 was assigned to Class W in another report, but the basis for this classification is unclear²⁰.

Uranium tetrafluoride was assigned Class Y from this work, and received the same classification by this author in an examination of the dissolution behavior of two commercial samples of UF_4 . This compound has been assigned to Class W in two reports^{19,20}, but the disagreement may well be due to differences in the thermal histories of the samples.

COMPARISON OF PLANT-SAMPLE CLASSIFICATIONS WITH EXPECTATIONS

At the front end of LWR-fuel plants, one would expect to incur airborne UF_6 and UO_2F_2 . This expectation was supported by the high percentage of Class D uranium in the sample collected at the UF_6 hydrolyzer of the Babcock and Wilcox plant and one of two sampling locations near the UF_6 hydrolyzer at the General Electric plant. The large amount of Class Y uranium found at the other sampling location may indicate that it receives airborne uranium from other parts of the General Electric plant.

The main airborne products expected at an ADU granulator or in the calciner feed are ammonium diuranate and uranium trioxide. The dissolution behavior of dust at such locations in all four plants was in agreement with this expectation. The products ranged from 45 to 72% D with the remainders being Class Y. This corresponds to the classification of ammonium diuranate that has been partially converted to uranium trioxide during the drying process. The calciner feed in a dry process stream, such as that at the General Electric plant, is expected to contain UO_2F_2 , U_3O_8 , UF_4 , and UO_2 . Since all of these except UO_2F_2 were found to be Class Y compounds in this study, a sample from this location would be expected to have both D and Y components, with the latter predominating. This was, in fact, the situation found.

At the discharge end of a calciner, the expected product is U_3O_8 , a Class Y compound. This was confirmed by studies on the dust samples from this location at the Babcock and Wilcox and General Electric plants. The 1-6% of Class D material probably represents incomplete conversion of $(NH_4)_2U_2O_7$ to U_3O_8 .

At the discharge end of the reduction kiln and at the fuel-pellet press, the expected product is UO_2 , a Class Y compound. This was confirmed by the dissolution behavior of the dust samples from such locations at the Exxon, Babcock and Wilcox, and General Electric plants.

Dust from UO_2 that has passed through a sintering furnace is expected to remain UO_2 but to be more resistant to dissolution. This was confirmed by the dissolution behavior of the dust samples from the sintering furnaces and pellet grinders of the plants.

At scrap recovery areas, uranium materials are heated in air to reoxidize UO_2 to U_3O_8 , and then the U_3O_8 is dissolved in nitric acid for reintroduction at the front end of the process line. Both Class Y U_3O_8 and Class D $UO_2(NO_3)_2$ are thus expected in this area, and the composition of dust in an air sample would depend on the exact location of the sampling system. This was confirmed in samples from three of the plants. The sample from the Exxon plant was 100% Y indicating only U_3O_8 was present, and this was confirmed by crystallographic analysis. The sample from Westinghouse plant was 30% D, 70% Y, suggesting the presence of both U_3O_8 and $UO_2(NO_3)_2$. A similar result, 61% D, 39% Y, was obtained from the sample collected in the analogous location of the Babcock and Wilcox plant. Closer to the actual scrap dissolver at this plant, airborne dust had the classification 91% D, 9% W, suggesting almost pure $UO_2(NO_3)_2$.

Samples collected at the air-recirculation intakes for the "Chem Room" in the General Electric plant provide an interesting insight into the composition of airborne dust from a major portion of the overall process; i.e., from hydrolysis of the UF_6 to formation of granulated UO_2 ready for the pellet presses. Since this plant runs the ADU process and its dry process in parallel lines on different sides of the room, it was also of interest to compare the overall classifications of dust samples in a direction at right

angles to the process streams. The results showed that the dissolution-rate classification of dust at these room-air intakes is independent of lateral position across the room and, perhaps coincidentally, is that of dust from the feed to the ADU calciner, i.e., 63% D, 37% Y.

REFERENCES

1. Task Group on Lung Dynamics for Committee II of the International Commission on Radiological Protection, "Deposition and Retention Models for Internal Dosimetry of the Human Respiratory Tract." Health Phys. 12: 173-206 (1966).
2. L. M. Steckel and C. M. West, Characterization of Y-12 Uranium Process Materials Correlated with In Vivo Experience. Y-1544A, Union Carbide Corporation, Oak Ridge Y-12 Plant, Oak Ridge, TN 37831 (1966).
3. N. Cooke and F. B. Holt, "The Solubility of Some Uranium Compounds in Simulated Lung Fluid." Health Phys. 27:69-77 (1974).
4. P. E. Morrow, F. R. Gibb, and L. Johnson, "Clearance of Insoluble Dust from the Lower Respiratory Tract." Health Phys. 10:543-555 (1964).
5. P. E. Morrow, F. R. Gibb, H. Davis, and M. Fisher, "Dust Removal from the Lung Parenchyma: An Investigation of Clearance Stimulants." Tox. and Appl. Pharm. 12:372-396 (1968).
6. J. R. Houston, D. L. Strenge, and E. C. Watson, DACRIN - A Computer Program for Calculating Organ Dose from Acute or Chronic Radionuclide Inhalation. BNWL-B-389, Pacific Northwest Laboratory, Richland, WA (1975).
7. K. Diem and C. Lentner, Ed., Documenta Geigy Scientific Tables, Seventh Edition, CIBA-GEIGY, Ltd., Basel, p. 523 (1970).
8. O. R. Moss, "Simulants of Lung Interstitial Fluid." Health Phys. 36: 447-448 (1979).
9. N. A. Dennis, Dissolution Rates of Yellowcake in Simulated Lung Fluids, M. S. Thesis, University of Pittsburgh, Pittsburgh, PA (1979).
10. D. R. Kalkwarf, Solubility Classification of Airborne Products from Uranium Ores and Tailings Piles. NUREG/CR-0530, PNL-2870, Pacific Northwest Laboratory, Richland, WA (1979).*
11. W. J. Maeck, G. L. Booman, M. C. Elliott, and J. E. Rein, "Spectrophotometric Extraction Methods Specific for Uranium." Anal. Chem. 31: 1130-1134 (1959).
12. C. J. Rodden, Ed., Selected Measurement Methods for Plutonium and Uranium in the Nuclear Fuel Cycle, Second Edition. TID-7092, Office of Information Services, U. S. Atomic Energy Commission (1972).
13. American Society of Testing and Materials, "Standard Test Methods for Microquantities of Uranium in Water by Fluorometry," Procedure D2907-75, 1979 Annual Book of ASTM Standards, Part 45, Nuclear Standards, pp. 783-788, American Society for Testing and Materials, Philadelphia, PA (1979).

* Available for purchase from the NRC/GPO Sales Program, U.S. Nuclear Regulatory Commission, Washington, DC 20555, and the National Technical Information Service, Springfield, VA 22161.

REFERENCES (continued)

14. T. T. Mercer, "On the Role of Particle Size in the Dissolution of Lung Burdens." Health Phys. 13:1211-1221 (1967).
15. I. A. McClaine, E. P. Bullwinkel, and J. C. Huggins, "The Carbonate Chemistry of Uranium: Theory and Applications." Proc. Intern. Conf. on Peaceful Uses of Atomic Energy, Geneva 1955, 8:26-37 (1956).
16. H. Füredi-Milhofer, Z. Despotovic', L. Devide', and M. Wrischer, "Precipitation and Hydrolysis of Uranium (VI) in Aqueous Systems-VII, Study of the Precipitates Formed in the Systems Uranyl Nitrate-Sodium Carbonate-Alkaline Earth Chlorides." J. Inorg. Nucl. Chem. 34: 1961-1969 (1972).
17. J. H. Gittus, Uranium. Butterworths, Washington, p. 41-42 (1963).
18. J. Chalabreysse, "Etude et Résultats d' Examens Effectués á la Suite d' une Inhalation de Composés dits Solubles d' Uranium Naturel." Radio-Protection 5: 1-17 and 305-310 (1970).
19. N. Cooke and F. B. Holt, "The Solubility of Some Uranium Compounds in Simulated Lung Fluid." Health Phys. 27:69-77 (1974).
20. R. E. Alexander, Applications of Bioassay for Uranium. WASH-1251, Directorate of Regulatory Standards, U. S. Atomic Energy Commission (1974).
21. W. D. Wilkinson, Uranium Metallurgy, Volume 1. Uranium Process Metallurgy. Interscience, New York, p. 25 (1962).
22. P. E. Morrow, F. R. Gibb, and H. D. Beiter, "Inhalation Studies of Uranium Trioxide." Health Phys. 23:273-280 (1972).
23. J. B. Hursh and N. L. Spoor, "Data on Man" in Uranium, Plutonium Transplutonium Elements, Eds. H. C. Hodge, J. N. Stannard, and J. B. Hursh. Springer-Verlag, Berlin, pp. 197-239 (1973).
24. P. E. Morrow, F. R. Gibb, and L. J. Leach, "The Clearance of UO₂ Dust from the Lungs Following Single and Multiple Inhalation Exposures." Health Phys. 12:1217-1223 (1966).

ACKNOWLEDGMENTS

The author wishes to thank and acknowledge the assistance of the following people in obtaining the plant samples used in this study: Mr. Paul Estey, Exxon Nuclear Co., Richland, WA; Mr. Ronald D. Corridoni, Babcock and Wilcox, Nuclear Fuels Division, Apollo, PA; Dr. G. Edward Powers, General Electric Co., Nuclear Energy Products Division, Wilmington, NC; and Mr. Richard K. Burklin, Westinghouse Electric Corporation, Nuclear Fuel Divisions, Columbia, SC. The author also gratefully acknowledges the assistance of other staff members at the Pacific Northwest Laboratory: Mr. Dean Robertson and Mr. Harvey Tenny, for conducting the microprobe and X-ray crystallographic samples; Mr. James Merril for assisting in the parametric resolution of the dissolution data; and particularly Mr. Charles Veverka for technical assistance in all phases of the work.

DISTRIBUTION

<u>No. of Copies</u>		<u>No. of Copies</u>	
	<u>OFFSITE</u>		<u>ONSITE</u>
	A. A. Churm DOE Patent Division 9800 S. Cass Avenue Argonne, IL 60439		<u>Pacific Northwest Laboratory</u>
265	U. S. Nuclear Regulatory Commission Division of Technical In- formation & Document Control 7920 Norfolk Avenue Bethesda, MD 20014	35	W. D. Felix D. R. Kalkwarf (25) R. W. Perkins L. C. Schwendiman Technical Information (5) Publishing Coordination (2)
2	DOE Technical Information Center Oak Ridge, TN 37830		
25	Dr. Lewis Battist U. S. Nuclear Regulatory Commission Office of Standards Develop- ment Washington, D. C. 20555		
	Mr. Paul Estey Exxon Nuclear Co. 2101 Horn Rapids Road Richland, WA 99352		
	Mr. Ronald D. Corridoni Babcock and Wilcox Co. Nuclear Materials Division 609 N. Warren Avenue Apollo, PA 15613		
	Dr. G. Edward Powers General Electric Co. Nuclear Energy Products Division P. O. Box 780 Wilmington, NC 28401		
	Mr. Richard K. Burklin Westinghouse Electric Corp. Nuclear Fuels Division Drawer R Columbia, SC 29205		

NRC FORM 335 (7-77)		U.S. NUCLEAR REGULATORY COMMISSION BIBLIOGRAPHIC DATA SHEET		1. REPORT NUMBER (Assigned by DDC) NUREG/CR-1428 PNL-3411	
4. TITLE AND SUBTITLE (Add Volume No., if appropriate) Solubility Classification of Airborne Uranium Products from LWR-Fuel Plants				2. (Leave blank)	
7. AUTHOR(S) D. R. Kalkwarf				5. DATE REPORT COMPLETED MONTH YEAR July 1980	
9. PERFORMING ORGANIZATION NAME AND MAILING ADDRESS (Include Zip Code) Pacific Northwest Laboratory Richland, WA 99352				DATE REPORT ISSUED MONTH YEAR August 1980	
12. SPONSORING ORGANIZATION NAME AND MAILING ADDRESS (Include Zip Code) Office of Standards Development U.S. Nuclear Regulatory Commission Washington, DC 20555				6. (Leave blank)	
10. PROJECT/TASK/WORK UNIT NO.				8. (Leave blank)	
11. CONTRACT NO. FIN No. B21239				13. TYPE OF REPORT	
15. SUPPLEMENTARY NOTES				PERIOD COVERED (Inclusive dates)	
14. (Leave blank)				16. ABSTRACT (200 words or less) Airborne dust samples were obtained from various locations within plants manufacturing fuel elements for light-water reactors, and the dissolution rates of uranium from these samples into simulated lung fluid at 37°C were measured. These measurements were used to classify the solubilities of the samples in terms of the lung clearance model proposed by the International Commission on Radiological Protection. Similar evaluations were performed for samples of pure uranium compounds expected as components in plant dust. The variation in solubility classifications of dust encountered along the fuel production lines is described and correlated with the process chemistry and the solubility classifications of the pure uranium compounds.	
17. KEY WORDS AND DOCUMENT ANALYSIS				17a. DESCRIPTORS	
17b. IDENTIFIERS/OPEN ENDED TERMS					
18. AVAILABILITY STATEMENT Unlimited				19. SECURITY CLASS (This report) Unclassified	
20. SECURITY CLASS (This page) Unclassified				21. NO. OF PAGES	
22. PRICE \$				23. PRICE	